Lifetimes, transition probabilities, and level energies in Fe I

T. R. O'Brian, M. E. Wickliffe, and J. E. Lawler

University of Wisconsin—Madison, Madison, Wisconsin 53706

W. Whaling

California Institute of Technology, Pasadena, California 91125

J. W. Brault

National Solar Observatory, Tucson, Arizona 85726

Received October 1, 1990; accepted December 13, 1990

We use time-resolved laser-induced fluorescence to measure the lifetime of 186 Fe I levels with energies between 25 900 and 60 758 cm^{-1}. Measured emission branching fractions for these levels yield transition probabilities for 1174 transitions in the range 225–2666 nm. We find another 640 Fe I transition probabilities by interpolating level populations in the inductively coupled plasma spectral source. We demonstrate the reliability of the interpolation method by comparing our transition probabilities with absorption oscillator strengths measured by the Oxford group [Blackwell *et al.*, Mon. Not. R. Astron. Soc. **201,** 595–602 (1982)]. We derive precise Fe I level energies to support the automated method that is used to identify transitions in our spectra.

1. INTRODUCTION

We recently demonstrated with Mo I an automated method for extracting a large number of atomic transition probabilities of modest precision from Fourier-transform spectra.[1] In the present paper we apply this method to a more important and better-known atom, Fe I, for which accurate gf values already exist against which we can test the results of our method. The method requires the radiative lifetime of many atomic levels—the more the better—with excitation energies distributed over the maximum possible range; in Section 2 we report the measurement by laser fluorescence of the lifetime of 186 Fe I levels between 25 900 and 60 758 cm^{-1}.

In Section 3 we report the automated measurement of emission branching fractions for the decay of these levels and determine transition probabilities for the decay channels. In Section 4 we use the transition probabilities to investigate the population of excited Fe I levels in the inductively coupled plasma (ICP) source and show that one can interpolate between levels of known lifetimes, and hence of known populations, to find the population of new levels of unknown lifetime. Once the population of a level is known, the transition probability can be found for every measurable transition by which the level decays. The two methods combined yield 1814 transition probabilities. We publish in this paper only a sample of the stronger lines; as in the case of Mo I, those who need the complete results may obtain them on request in machine-readable form.

To establish the soundness of our population method and validate the uncertainty estimates that we assign, in Section 5 we compare Fe I transition probabilities measured by the lifetime and the population methods with the precise absorption oscillator strengths measured by Blackwell *et al.*[2] With the reliability of our results confirmed, we proceed to use our values to test the precision of two other collections of Fe I transition probabilities: the 1985 National Institute of Standards and Technology (NIST) compilation[3] (2092 lines) and the semiempirical values of Kurucz[4] (~10^6 lines). To support the automated line-identification process, in Section 6 we present improved Fe I level energies determined from our spectra, and we compare our level energies with those in the NIST *Atomic Energy Levels*[5] (AEL).

2. LEVEL LIFETIMES

Radiative lifetimes for 186 levels of Fe I were measured with time-resolved laser-induced fluorescence on a slow Fe atomic beam. This approach has proved highly reliable for measurements on neutral and singly ionized atoms.[6] Selective laser excitation eliminates the cascading problem that plagues beam-foil time-of-flight measurements. The beam environment eliminates errors that are due to radiation trapping and collisional quenching.

Figure 1 is a schematic of the experiment. The atomic or ionic beam source is based on a low-pressure large-bore hollow-cathode discharge. This versatile sputter source produces intense atomic or ionic beams of any metallic element. The hollow cathode is used to form uncollimated atomic or ionic beams by sealing one end of the cathode except for a 1.0-mm-diameter opening, flared outward at 45°. The hollow cathode and the scattering chamber are at ground potential. Ar, the sputtering gas, flows continuously into the hollow-cathode discharge. The scattering chamber is sealed from the hollow-cathode discharge, except for the nozzle, and is maintained at a much lower pressure than the discharge by a 10-cm diffusion pump. The Ar pressure in the discharge is typically 0.4 Torr, while the scattering chamber pressure is 10^{-4} Torr. The hollow-cathode discharge is operated with dc currents of

0740-3224/91/061185-17$05.00

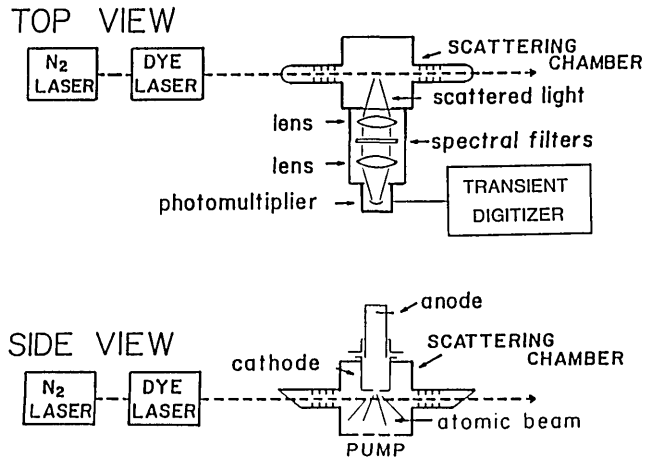

Fig. 1. Schematic diagram of the laser fluorescence apparatus.

20–200 mA and with 5-μs pulses as large as 25 A. When operated in a pulse mode the discharge current is maintained at 50 mA between pulses by the dc supply. A more detailed description of the source, including a drawing showing dimensions and materials, has been published.[7]

The atomic beam is crossed by a pulsed dye-laser beam 1.0 cm from the nozzle. The dye laser, pumped by a pulsed N_2 laser, produces an optical pulse of 3-ns duration (FWHM) with a 0.2-cm^{-1} bandwidth and a peak power of up to 40 kW. Potassium dihydrogen phosphate (KDP) and β-barium borate (BBO) crystal frequency doublers extend the dye laser tuning range to 205 nm in the UV. The fluorescence is detected along an axis orthogonal to the atomic beam and laser beam. In order to minimize scattered light, several sets of light baffles are arranged along the laser-beam axis inside the Brewster windows that pass the laser beam into and out of the scattering chamber. Two independently tuned dye lasers were used to excite six of the high-lying even-parity levels by two-step laser excitation.

Two lenses composing an $f/1$ system with unity magnification are used to collect the laser-induced fluorescence. The fluorescent light is approximately collimated between the two lenses. Interference filters or dye filters may be inserted between the lenses. Occasionally, branching ratios are favorable for observing fluorescence at a wavelength that is much different from the laser wavelength. Filters are used to block all scattered laser light and to isolate the laser-induced fluorescence whenever possible. Repopulation by radiative cascade from higher-lying levels is not a problem because of the highly selective laser excitation. Filters are used to block emission from lower-lying levels, which are populated by radiative cascade. High-lying even-parity levels are prone to produce cascade fluorescence from lower odd-parity levels.

The detection system is composed of a photomultiplier, a delay cable, and either a boxcar averager or a transient digitizer. The bias resistors of the 1P28A photomultiplier are bypassed with capacitors in order to ensure good linearity at large peak currents; small damping resistors are included to reduce ringing. All components are wired for low inductance and fast response. The 0.1-ns rise-time delay cable is necessary for synchronization of electronic components when the boxcar averager is used. The window width of the PAR-163/162 boxcar averager is 75 ps. Most of the 6070 fluorescence decay curves for this study were logged with a Tektronix 7912AD transient digitizer, shown in Fig. 1, since its data collection rate is a hundred times that of the boxcar. The digitizer has an analog bandwidth of 0.5 GHz and a sampling rate of 200 GHz. We often compared the two data-logging systems in order to test for small systematic errors. Measuring well-known He I and Be I lifetimes tests the accuracy of the experiment and confirms that lifetimes as short as 2 ns can be accurately measured.[8] A trigger generator provides an adjustable delay between the current pulse to the hollow cathode and the laser pulse. Pulsing the atomic beam source has two advantages: It produces a much higher flux of atoms, especially in high metastable levels (while still maintaining low average discharge current), and it permits extensive studies of potential error in very long (~2-μs) lifetimes that arises from atoms' escaping from the observation region before radiating.[9] Error due to atoms' escaping from the observation region before radiating is negligible in this Fe I experiment.

We routinely use more than one transition for laser excitation of a level. This redundancy provides a check that the chosen transitions have been correctly classified, are correctly identified in the experiment, and are unblended. Typically these independent measurements agree to a few percent. One of the most interesting discoveries during this investigation is that long-lived ($\geq 10^{-4}$ s) odd-parity levels have useful populations in the atomic beam. All but six of the lifetimes for high-lying even-parity levels were measured with single-step laser excitation. Two-step excitation, which was necessary for the six levels from the e^5H and e^3H terms, confirms the classification of lines connected to these levels, because the fluorescence from these levels is extinguished when either laser beam is interrupted.

The dynamic range of this experiment extends from 2-ns lifetimes, where it is limited by the electronic bandwidth of the detection apparatus, to 2-μs lifetimes, where it is limited by atoms' escaping from the observation region before radiating. Other possible systematic errors from radiation trapping, collisional quenching, or Zeeman quantum beats are unimportant. Tests for radiation trapping are routinely performed by variation of the atomic beam intensity. Many such tests on strong resonance transitions were performed, and radiation trapping of metal atom transitions was not detected. Collisional quenching is not a problem because of the low scattering chamber pressure (10^{-4} Torr of Ar). The absence of collisional quenching is confirmed by variation of the scattering chamber pressure when long lifetimes are measured. Zeeman quantum beats are avoided by measurement of short (<300-ns) lifetimes in zero magnetic field (<20 mG) and long (>300-ns) lifetimes in a high (30 G) field. We claim a total uncertainty that is the greater of $\pm 5\%$ or ± 0.2 ns in our lifetime measurements. This uncertainty includes both systematic and random error. Our lifetime measurements and the transitions used for laser excitation are listed in Table 1.

A comparison of our measurements with those of previous investigations, especially laser-induced fluorescence measurements, provides convincing evidence that our total uncertainty is a realistic estimate of both systematic and random error. In Table 1 we list (on the line below our

Table 1. Radiative Lifetime of Fe I Levels*

Level	Energy (cm^{-1})	Transitions (nm)	τ (ns)
$z^5D^o_4$	25899.986	385.99, 539.71	78.2
		89.0(4.8)[a], 81.4(5.0)[b], 78.5(2.0)[c]	
$z^5D^o_3$	26140.177	388.63, 532.80	81.1
		87.2(4.8)[a], 83.5(5.0)[b]	
$z^5D^o_2$	26339.694	385.64, 537.15	84.5
		94.7(5.3)[a], 82.3(5.0)[b]	
$z^5D^o_1$	26479.376	387.86, 540.58	86.3
		91.2(5.0)[a], 83.5(5.0)[b]	
$z^5D^o_0$	26550.474	389.57, 543.45	88.5
		88.6(5.0)[a], 85.6(5.0)[b]	
$z^5F^o_5$	26874.546	501.21, 512.74	60.5
		62.4(4.2)[b], 61.0(1.0)[c]	
$z^5F^o_4$	27166.816	505.16, 514.29	63.6
			63.7(4.0)[b]
$z^5F^o_3$	27394.687	499.41, 508.33	66.3
			65.1(4.0)[b]
$z^5F^o_2$	27559.580	504.11, 515.19	67.9
$z^5F^o_1$	27666.344	507.97, 512.37	68.8
			64.6(4.0)[b]
$z^3D^o_3$	31322.610	319.17, 532.85	254
$z^3D^o_2$	31686.349	319.70, 534.10	245
$z^3D^o_1$	31937.323	322.91, 527.04	237
$y^5D^o_4$	33095.937	382.04, 388.71	5.9
$y^5D^o_3$	33507.119	382.59, 387.80	5.7
			6.1(5)[d]
$y^5F^o_5$	33695.394	460.29	7.9
			8.16(30)[a]
$y^5D^o_2$	33801.568	383.42, 387.25	6.5
$z^3P^o_2$	33946.929	385.08, 387.60	38.3
		37.0(2.2)[b], 38.6(2.0)[d]	
$y^5D^o_1$	34017.099	384.04, 386.55	5.8
			6.1(2)[d]
$y^5F^o_4$	34039.512	453.12, 465.45	7.7
			8.29(30)[a]
$y^5D^o_0$	34121.597	385.00	5.8
			5.9(2)[d]
$y^5F^o_3$	34328.748	459.27, 468.03	7.7
			7.92(25)[a]
$z^3P^o_1$	34362.869	379.01, 381.45	99.6
		94.1(5.5)[b], 112(11)[d]	
$y^5F^o_2$	34547.206	454.70, 463.29	7.7
			8.00(30)[a]
$z^3P^o_0$	34555.592	296.94, 378.67	112
		108.0(7.0)[b], 111.5(5.0)[d]	
$y^5F^o_1$	34692.143	460.20	7.8
			7.86(25)[a]
$z^5G^o_5$	34782.417	438.36	11.6
			11.7(7)[b]
$z^5G^o_4$	35257.321	429.41, 440.48	10.8
			11.2(7)[b]
$z^3G^o_5$	35379.204	427.18	10.2
$z^5G^o_3$	35611.621	433.70, 441.51	10.2
			10.3(6)[b]
$z^3G^o_4$	35767.560	420.20, 430.79	10.8
$z^5G^o_2$	35856.397	436.79	9.9
$z^3G^o_3$	36079.368	425.08, 432.58	11.7
$y^3F^o_4$	36686.172	404.58, 414.39	9.6
			9.11(16)[e]
$y^5P^o_3$	36766.963	403.26, 520.23	5.7
$y^5P^o_2$	37157.561	406.45, 509.87	6.0
$y^3F^o_3$	37162.743	406.36, 413.21	9.5
			9.06(13)[e]
$y^5P^o_1$	37409.549	507.92, 513.15	6.2
$y^3F^o_2$	37521.157	400.52, 407.17	9.6
			9.06(16)[e]
$y^3D^o_3$	38175.348	381.58, 390.30	7.1
$y^3D^o_2$	38678.034	382.78, 388.85	7.1
$y^3D^o_1$	38995.731	384.11	7.2
$x^5D^o_4$	39625.799	452.86	2.6
$x^5D^o_3$	39969.848	449.46	2.6
$y^7P^o_2$	40052.018	255.26, 444.28	444
$y^7P^o_3$	40207.090	248.64, 251.24	146
$x^5D^o_2$	40231.332	448.23	2.6
$x^5F^o_5$	40257.307	248.33	2.0
$x^5D^o_1$	40404.513	444.77	2.6
$y^7P^o_4$	40421.938	247.32	309
$x^5D^o_0$	40491.279	443.06	2.6
$x^5F^o_4$	40594.427	248.81	2.0
$x^5F^o_3$	40842.149	247.29	2.0
$z^5S^o_2$	40894.986	248.74, 428.24	36.9
$x^5F^o_2$	41018.046	247.98	2.0
$x^5F^o_1$	41130.594	248.42, 248.98	2.0
$x^5P^o_3$	42532.736	237.36, 239.00	46.6
$y^5G^o_6$	42784.350	278.81	16.9
e^7D_5	42815.851	426.05	8.3
$x^5P^o_2$	42859.773	237.14, 238.18	30.4
$y^5G^o_5$	42911.911	277.82, 281.33	23.1
$z^5H^o_5$	42991.693	280.70	72.1
$y^5G^o_4$	43022.979	280.45, 283.24	28.6
$x^5P^o_1$	43079.019	237.45	93.0
$z^5H^o_4$	43108.913	279.78, 282.56	55.2
$y^5G^o_3$	43137.483	282.33	20.5
e^7D_4	43163.321	423.59, 427.12	8.5
$y^5G^o_2$	43210.020	281.75, 283.81	20.8
$z^5H^o_3$	43325.960	282.88	391
e^7D_3	43434.624	418.78, 425.01	8.4
$w^5D^o_4$	43499.503	273.36, 385.26	7.4
e^7D_2	43633.529	418.70, 423.36	8.4
e^7D_1	43763.977	419.14, 421.03	8.4
$w^5D^o_3$	43922.665	273.55, 381.63	8.5
$^5D^o_4$	44022.521	229.25, 272.80	95.9
$^5D^o_3$	44166.200	230.01, 274.36	68.3
$w^5D^o_2$	44183.622	274.23, 316.14	8.9
$^5F^o_5$	44243.682	225.95, 267.91	39.0
$^5F^o_2$	44285.451	229.38, 230.36	54.0
$^5F^o_1$	44378.338	229.87, 230.34	41.7

(continued overleaf)

Table 1. Continued

Level	Energy (cm^{-1})	Transitions (nm)	τ (ns)
$w^5D_1^o$	44411.153	274.45, 275.73	10.5
$^5F_4^o$	44415.069	227.21, 269.91	41.2
$w^5D_0^o$	44458.930	229.44, 275.37	11.5
$y^5S_2^o$	44511.807	226.71, 271.78	13.6
$^5F_3^o$	44551.333	227.99, 268.92	41.6
$^5D_2^o$	44664.074	228.37, 270.66	31.7
$^5D_1^o$	44760.741	226.91, 271.84	21.4
$^5D_0^o$	44826.880	227.52, 272.61	16.3
$x^3D_3^o$	45220.674	223.12, 264.16	23.0
$x^3D_2^o$	45281.828	225.19, 388.55	21.3
$y^3G_5^o$	45294.841	260.57, 385.92	55.7
$y^3G_4^o$	45428.397	387.38, 389.90	64.0
$x^3D_1^o$	45551.760	306.82, 384.52	19.8
$y^3G_3^o$	45562.970	266.04, 306.71	67.2
$x^5G_6^o$	45608.358	258.45	31.4
$x^5G_5^o$	45726.126	257.67, 260.68	28.1
$x^5G_4^o$	45833.219	262.35	26.8
$x^5G_3^o$	45913.498	261.80, 263.58	26.4
$x^5G_2^o$	45964.953	263.22, 264.40	26.8
$z^3I_7^o$	45978.002	376.01	191
$z^3I_6^o$	46026.965	378.60	200
$z^3I_5^o$	46135.812	379.43	211
$z^3H_6^o$	46982.315	249.59, 395.67	43.3
$z^3H_5^o$	47008.366	252.25, 399.74	35.9
$z^3H_4^o$	47106.479	251.63, 284.57, 402.19	36.5
$w^5G_6^o$	47363.371	389.79	60.0
$w^5G_5^o$	47420.224	246.89, 249.65	20.2
$w^5G_4^o$	47590.042	248.60, 250.79	35.5
$w^5G_3^o$	47693.236	251.77, 389.08	41.0
$x^3G_4^o$	47812.114	244.52, 283.59	44.8
$w^5G_2^o$	47831.149	251.96, 390.79	34.2
$x^3G_3^o$	47834.215	249.26, 250.88	102
$x^3G_5^o$	47834.547	244.39, 247.10	43.6
$^5H_5^o$	48231.275	242.04, 377.03	175
$^5H_4^o$	48361.875	279.24, 379.22	139
$^5H_3^o$	48475.680	281.55, 364.37, 381.19	130
$y^3H_6^o$	49434.159	389.75	11.5
$v^3G_5^o$	49460.896	266.70, 389.34	11.4
$y^3H_5^o$	49604.422	265.68, 387.17	11.6
$v^3G_4^o$	49627.878	269.70, 391.91	11.3
$y^3H_4^o$	49726.985	268.98, 390.39	11.3
$v^3G_3^o$	49850.584	271.05, 391.86	11.6
e^7F_6	50342.127	322.58	5.6
f^7D_5	50377.905	324.42	5.7
e^5G_6	50522.940	320.71	13.0
			13.0(8)[b], 13.0(7)[f]
e^5G_5	50703.865	318.86, 321.02	11.5
			11.7(7)[b]
f^7D_4	50807.993	321.96	6.2
e^7F_5	50833.432	317.54	6.7
f^7D_3	50861.816	321.40	7.4
e^7G_6	50967.826	316.20	6.5
e^5G_4	50979.574	318.21	12.8
			13.0(8)[b]
f^7D_2	50998.641	321.59	7.5
f^7D_1	51048.100	321.08	7.0
e^7F_3	51148.857	316.50, 318.46, 320.05	8.3
e^5S_2	51148.905	321.15	9.6
e^7F_4	51192.269	318.02	6.5
e^7F_1	51207.993	320.54	5.9
e^5G_3	51219.012	315.80, 319.33	9.5
e^7G_5	51228.548	315.70	7.8
e^7F_2	51331.050	318.19	7.4
e^7G_4	51334.905	316.59	7.5
e^5G_2	51370.141	316.23, 318.88	10.3
e^7G_3	51460.514	315.33, 316.89	6.7
f^5F_4	51461.669	315.32	12.7
e^7G_2	51539.718	317.17	6.7
e^7S_3	51570.094	314.25, 315.79	7.3
f^5F_3	51604.100	315.45	14.8
$w^3H_6^o$	52431.438	302.56, 379.75	8.9
$y^3I_6^o$	52513.552	303.93	11.2
$w^3H_5^o$	52613.083	303.01, 380.67	9.1
$y^3I_7^o$	52654.983	300.53	10.2
$w^3H_4^o$	52768.736	303.12, 382.43	9.3
$y^3I_5^o$	52898.990	300.41	10.7
e^5H_6	53352.980	538.34 + 438.36	12.8
			12.8(8)[b]
g^7D_5	53800.856	290.19, 320.93	22.7
e^3H_6	53840.614	541.52 + 427.18	12.8
e^5H_5	53874.251	537.00 + 440.48	12.9
			13.4(9)[b]
$t^3G_5^o$	53983.294	309.82	12.0
g^7D_4	54124.735	289.25, 290.89	24.3
e^5H_4	54237.156	536.75 + 441.51	12.9
$t^3G_4^o$	54237.409	288.80, 307.40	10.9
e^3H_5	54266.706	540.42 + 430.79	13.0
e^3H_4	54555.413	541.09 + 432.58	13.7
$t^3G_3^o$	54600.345	306.65, 309.02	10.1
g^7D_2	54611.711	286.82, 318.18	22.8
g^7D_1	54747.608	286.98, 317.34	23.0
$^3H_4^o$	55446.004	280.36, 301.15	17.0
$^3H_6^o$	55489.734	276.93, 296.00	11.1
$^3H_5^o$	55525.555	278.43, 295.69	9.0
$u^3H_6^o$	56333.955	270.60, 288.78	19.8
$u^3H_5^o$	56382.656	271.94, 290.75	12.6
$u^3H_4^o$	56423.276	271.64, 272.88	10.4
$u^3F_4^o$	56592.695	271.63, 278.07, 304.7	9.9
$u^3F_3^o$	56783.316	278.40, 306.05	11.4
$x^3I_7^o$	57027.505	265.62	17.2
$x^3I_6^o$	57070.165	266.95	17.4
$x^3I_5^o$	57104.205	307.32, 328.03	17.2
$t^3F_4^o$	57550.005	270.86, 278.98	9.2
$t^3F_3^o$	57641.005	254.62, 270.19	7.9
$t^3F_2^o$	57708.742	271.41, 272.62	8.9
$^3I_7^o$	58792.247	253.72	2.7
$^3I_6^o$	58946.730	254.21	2.0
$^3I_5^o$	59085.825	254.39	2.0
$t^3H_6^o$	60365.631	243.97	2.1
$t^3H_5^o$	60549.110	244.26	2.1
$t^3H_4^o$	60757.600	244.01, 249.20	2.1

*The uncertainty of our value in the last column is the larger of ±5% or ±0.2 ns. Other values measured by laser fluorescence are listed below our result. The uncertainty in the last digit(s) of the other values appears in parentheses.

[a] Ref. 10, [b] Ref. 11, [c] Ref. 12, [d] Ref. 13, [e] Ref. 14, [f] Ref. 15.

value) lifetimes for 31 levels that have been measured by other groups[10–15] using laser-induced fluorescence. The uncertainty in the last digit(s) of each entry is enclosed in parentheses following the entry. Our measurements of these level lifetimes agree within the combined error estimates in essentially every case.

3. TRANSITION PROBABILITIES FROM LEVEL LIFETIMES

Given the radiative lifetime τ_u of excited level u, the transition probability A_{ul} for the transition from level u to level l is given by

$$A_{ul} = \mathrm{BF}_{ul}/\tau_u, \tag{1}$$

where BF_{ul} is the emission branching fraction for the transition. We find BF_{ul} from the line intensities $\mathrm{BF}_{ul} = I_{ul}/\Sigma_{l'} I_{ul'}$, where I is the intensity (in photons per second) of a line after correction for spectrometer response and the sum is taken over all lower levels l' to which the upper level u decays. The spectrophotometry of the line intensities is standard and has been described in detail in Ref. 1; only a summary of the significant parameters will be presented here.

Fourteen spectra, all recorded on the 1-m Fourier-transform spectrometer[16] (FTS) at the National Solar Observatory, Kitt Peak, were measured with the automated DECOMP program that fits a Voigt profile to an observed line to find the line-center wave number and the integrated line area. Nine of the spectra were recorded with a hollow-cathode source[17] operating at a few Torr of pressure of Ar, Ar + Ne, or Ar + He and at source power levels between 17 and 140 W/cm^3 of cathode cavity. Si diodes (250–1000 nm), InSb diodes (1000–5000 nm), and solar-blind photoelectric detectors (225–300 nm) were used for different spectral ranges.

The response of the spectrometer system was determined internally for each spectrum from the observed intensity of Ar lines whose true intensity ratios are known, as described in Ref. 1. We extended this branching-ratio method for calibrating spectrometer response into the IR in this experiment by using He line pairs that span the range 400–3300 nm to calibrate a broad range spectrum in which an InSb IR detector was installed on one of the FTS exit channels and a UV Si detector on the other. The use of the two exit channels of the FTS as independent spectrometers was described by Wiese *et al.*[18] The He transition strengths were calculated most recently by Fernley *et al.*,[19] and we used their values for this calibration.

Five spectra measured for this experiment were excited in an inductively coupled Ar plasma source that contained a trace of $Fe(CO)_5$ and operated at 27 MHz, 1 kW, and 600 Torr of Ar. The distinctive features of the ICP spectrum were discussed in Ref. 1, and we mention only two that we exploit in this work: the broad linewidth (from Doppler broadening at ~7000 K) and the distribution of excited-level populations, which we discuss in Section 5. Emission spectrophotometry is always threatened by self-absorption, a threat that increases as the linewidth narrows. We found that the extremely broad lines of the ICP source are much less prone to self-absorption than are those of the hollow-cathode source, and we measured the intensity of strong decay channels on the ICP spectra whenever possible.

The population of excited levels in the ICP falls off exponentially as the excitation increases, so that the ICP spectrum is most useful for lines from lower levels, which are, fortunately, those most likely to be self-absorbed. To guard against self-absorption of lines from higher levels that could be measured only on the hollow-cathode spectrum, we used the standard technique of decreasing the source power until line-intensity ratios held constant. We also used an attractive feature of the DECOMP program: After fitting the parameers of a Voigt profile to the observed line, DECOMP displays the residual difference between the observed line and the Voigt profile. Self-absorption produces a characteristic symmetrical double-humped residual that is easily recognized long before any sign of self-absorption is apparent in the experimental line shape.

Although the ICP is an Ar plasma, Ar lines are not prominent in our ICP spectra and cannot be used to calibrate the response. Instead we used well-known Fe branching ratios to establish reference points on the response curve and filled in between these points with the observed response to a commercial W-ribbon radiance standard.

Line-intensity ratios on the 14 measured spectra were intercompared, averaged, and combined so we could find the branching fractions for levels of measured lifetimes. We believe that we have included in the sum in Eq. (1) all significant transitions, because we chose for lifetime measurement only levels that are known or expected to decay within the 4000–45000 cm^{-1} range of our spectra. Our expectation derives from the semiempirical branching ratios computed by Kurucz[4]; in Section 5 we test his theoretical predictions against experiment and find their accuracy to be adequate for this purpose.

With the radiative lifetimes of Table 1, our experimental branching fractions yield 1174 transition probabilities. A sample of these results are shown in Table 2. The fractional uncertainty $\pm\Delta A/A$ in the transition probability shown in parentheses for each line includes contributions from the uncertainty in the lifetime (5–10%), from the uncertainty ΔI in each line intensity included in the braching fraction, and from the uncertainty in the response function. For ΔI we use the empirical function of the signal-to-noise ratio deduced by Faires *et al.*[20] The response function $R(\lambda)$ contributes to the uncertainty $\Delta\mathrm{BF}$ (and hence to ΔA) in a complex way because it is only the relative response $[R(\lambda_l)/R(\lambda_{l'})]$ that is significant. The uncertainty in this ratio increases as the separation $\lambda_l - \lambda_{l'}$ increases. We have assumed a linear dependence on line separation:

$$\Delta[R(\lambda_l)/R(\lambda_{l'})] = 10^{-5}(\lambda_l - \lambda_{l'})[R(\lambda_l)/R(\lambda_{l'})],$$

with a proportionality constant of 0.001% per wave number, based on our experience with the branching-ratio method for calibrating spectrometer response. With this assumption the response function makes by far the largest contribution to the ΔA for lines that are far removed from the strongest decay channels. We test the reliability of our uncertainty estimates in Section 5.

Table 2. Transition Probability for 478 Strong Lines in Fe I*

Vacuum Waveno.	λ (nm)	Trans. Prob. ($10^7 s^{-1}$)		Upper Level	Lower Level	
12161.550	822.0376	1.69	12%	e^5F_5	$z^5G^o_6$	P
13310.107	751.1019	1.35	±9%	e^5F_5	$y^5F^o_5$	P
17894.508	558.6756	2.19	9%	e^5D_3	$z^5F^o_4$	P
18461.410	541.5199	7.68	5%	e^3H_6	$z^3G^o_5$	L
18476.044	541.0910	6.33	5%	e^3H_4	$z^3G^o_3$	L
18499.146	540.4153	6.92	5%	e^3H_5	$z^3G^o_4$	L
18570.564	538.3369	7.81	5%	e^5H_6	$z^5G^o_5$	L
18616.929	536.9962	7.22	5%	e^5H_5	$z^5G^o_4$	L
18625.583	536.7467	7.13	7%	e^5H_4	$z^5G^o_3$	L
18634.595	536.4871	5.60	12%	e^5H_3	$z^5G^o_2$	P
18982.460	526.6555	1.10	7%	e^7D_4	$z^7P^o_3$	L
19104.398	523.2940	1.94	5%	e^7D_5	$z^7P^o_4$	L
19126.613	522.6862	1.36	7%	e^7D_2	$z^7P^o_2$	L
19253.763	519.2344	1.34	6%	e^7D_3	$z^7P^o_3$	L
19257.061	519.1455	2.32	7%	e^7D_1	$z^7P^o_2$	L
19934.849	501.4942	2.64	13%	e^3D_2	$z^3F^o_3$	P
20053.567	498.5253	1.48	9%	e^3D_2	$z^3D^o_2$	P
20165.436	495.7597	4.22	5%	e^7D_5	$z^7F^o_6$	L
20166.650	495.7298	1.18	7%	e^7D_4	$z^7F^o_4$	L
20317.455	492.0503	3.58	6%	e^7D_4	$z^7F^o_5$	L
20323.688	491.8994	1.79	7%	e^7D_3	$z^7F^o_3$	L
20437.953	489.1492	3.08	5%	e^7D_3	$z^7F^o_4$	L
20441.033	489.0755	2.25	5%	e^7D_2	$z^7F^o_2$	L
20493.595	487.8211	1.21	5%	e^7D_1	$z^7F^o_0$	L
20519.141	487.2138	2.54	5%	e^7D_1	$z^7F^o_1$	L
20522.593	487.1318	2.44	5%	e^7D_2	$z^7F^o_3$	L
20571.481	485.9741	1.62	6%	e^7D_1	$z^7F^o_2$	L
22368.213	446.9376	1.59	17%	e^5P_3	$z^5P^o_2$	P
22382.355	446.6552	1.20	6%	$x^3D^o_3$	b^3P_2	L
22643.069	441.5123	1.17	6%	$z^5G^o_3$	a^3F_2	L
22696.388	440.4750	2.72	5%	$z^5G^o_4$	a^3F_3	L
22806.179	438.3545	5.09	5%	$z^5G^o_5$	a^3F_4	L
23103.691	432.7096	1.12	9%	$y^1D^o_2$	a^1D_2	P
23110.816	432.5762	5.16	5%	$z^3G^o_3$	a^3F_2	L
23206.628	430.7902	3.38	6%	$z^3G^o_4$	a^3F_3	L
23253.412	429.9235	1.29	5%	e^7D_5	$z^7D^o_4$	L
23344.807	428.2403	1.21	5%	$z^5S^o_2$	a^5P_3	L
23402.966	427.1761	2.23	6%	$z^3G^o_5$	a^3F_4	L
23406.291	427.1154	1.87	6%	e^7D_4	$z^7D^o_3$	L
23464.961	426.0474	3.99	7%	e^7D_5	$z^7D^o_5$	L
23522.129	425.0119	2.20	6%	e^7D_3	$z^7D^o_2$	L
23537.048	424.7425	1.94	9%	e^5G_5	$z^5F^o_4$	L
23584.887	423.8810	2.41	5%	e^5G_4	$z^5F^o_3$	L
23600.883	423.5937	2.00	6%	e^7D_4	$z^7D^o_4$	L
23613.894	423.3603	1.96	6%	e^7D_2	$z^7D^o_1$	L
23648.393	422.7427	5.30	7%	e^5G_6	$z^5F^o_5$	L
23659.431	422.5454	1.65	6%	e^5G_3	$z^5F^o_2$	L
23688.090	422.0342	1.83	12%	$x^3P^o_0$	c^3P_1	P
23693.601	421.9360	2.88	5%	$y^3I^o_6$	a^1H_5	L
23703.797	421.7545	2.46	6%	e^5G_2	$z^5F^o_1$	L
23744.342	421.0344	1.48	9%	e^7D_1	$z^7D^o_1$	L
23807.946	419.9095	4.92	9%	$z^1H^o_5$	a^1G_4	P
23810.561	419.8634	1.25	9%	e^5G_2	$z^5F^o_2$	L
23812.758	419.8247	1.47	5%	e^5G_4	$z^5F^o_4$	L
23829.318	419.5329	1.11	8%	e^5G_5	$z^5F^o_5$	L
23851.482	419.1431	2.73	10%	e^7D_1	$z^7D^o_2$	L
23872.186	418.7795	1.68	±6%	e^7D_3	$z^7D^o_4$	L
23876.499	418.7039	2.33	6%	e^7D_2	$z^7D^o_3$	L
23906.669	418.1755	2.32	9%	$^5D^o_3$	b^3P_2	P
23941.700	417.5636	1.14	9%	$^3D^o_2$	b^3P_1	P
24044.520	415.7780	2.18	5%	f^5F_3	$z^5F^o_2$	L
24050.193	415.6799	1.20	9%	$^3D^o_2$	b^3P_2	P
24061.732	415.4805	1.40	7%	e^7G_5	$z^5F^o_4$	L
24063.509	415.4499	2.64	10%	$y^3P^o_1$	b^3P_2	P
24066.980	415.3899	2.05	5%	f^5F_4	$z^5F^o_3$	L
24125.240	414.3868	1.33	5%	$y^3F^o_4$	a^3F_3	L
24127.880	414.3414	2.70	9%	$y^1G^o_4$	a^1G_4	P
24165.303	413.6998	2.75	9%	$y^1D^o_2$	a^1P_1	P
24178.863	413.4678	1.25	11%	$^3D^o_3$	b^3P_2	P
24194.191	413.2058	1.18	5%	$y^3F^o_3$	a^3F_2	L
24220.277	412.7608	1.43	9%	$^3D^o_1$	b^3P_0	P
24273.572	411.8545	4.96	9%	$z^1I^o_6$	a^1H_5	P
24325.211	410.9802	1.51	9%	$^3D^o_1$	b^3P_1	P
24338.911	410.7488	1.74	9%	$^5D^o_1$	b^3P_2	P
24523.147	407.6629	1.32	10%	f^5D_4	$z^5D^o_4$	P
24540.401	407.3763	1.68	10%	f^5D_1	$z^5D^o_2$	P
24552.605	407.1738	7.89	5%	$y^3F^o_2$	a^3F_2	L
24575.300	406.7978	1.51	9%	e^7P_4	$z^5D^o_4$	P
24601.810	406.3594	6.66	5%	$y^3F^o_3$	a^3F_3	L
24608.793	406.2441	1.85	11%	$y^3S^o_1$	b^3P_1	P
24709.935	404.5812	8.71	5%	$y^3F^o_4$	a^3F_4	L
24902.472	401.4531	1.53	11%	$z^1X^o_3$	a^1G_4	P
24960.224	400.5242	2.17	5%	$y^3F^o_2$	a^3F_3	L
25009.238	399.7392	1.26	5%	$z^3H^o_5$	a^3G_4	L
25139.911	397.6614	1.20	11%	$^3D^o_2$	a^1P_1	P
25186.506	396.9257	2.26	5%	$y^3F^o_3$	a^3F_4	L
25198.165	396.7421	1.52	9%	$u^3G^o_3$	b^3H_4	P
25264.407	395.7018	1.67	5%	f^5F_3	$z^5D^o_2$	L
25266.585	395.6677	1.22	5%	$z^3H^o_6$	a^3G_5	L
25268.000	395.6455	1.76	9%	$u^3G^o_5$	b^3H_6	P
25301.842	395.1163	4.29	10%	$y^1D^o_2$	a^3D_1	P
25317.146	394.8775	2.08	9%	$u^3G^o_4$	b^3H_5	P
25321.499	394.8096	1.31	7%	f^5F_4	$z^5D^o_3$	L
25400.524	393.5812	1.14	12%	$v^5F^o_2$	b^3P_2	P
25464.388	392.5941	1.67	12%	$x^3P^o_1$	b^3P_0	P
25511.822	391.8642	1.17	11%	$v^3G^o_3$	b^3G_3	L
25513.295	391.8415	4.23	13%	$x^3P^o_0$	b^3P_1	P
25614.417	390.2946	2.26	5%	$y^3D^o_3$	a^3F_3	L
25686.934	389.1927	2.71	15%	$^3P^o_1$	a^1P_1	P
25707.444	388.8822	1.95	15%	$w^3P^o_1$	c^3P_2	P
25709.483	388.8514	2.50	5%	$y^3D^o_2$	a^3F_2	L
25744.132	388.3280	1.28	13%	$u^3D^o_3$	a^3D_3	P
25774.354	387.8726	5.34	11%	$^1P^o_1$	a^3D_1	P
25815.785	387.2501	1.14	9%	$y^5D^o_2$	a^5F_2	L
25851.066	386.7216	3.16	10%	$w^3P^o_2$	c^3P_2	P
25862.387	386.5523	1.67	8%	$y^5D^o_1$	a^5F_1	L
25966.886	384.9967	6.16	7%	$y^5D^o_0$	a^5F_1	L
25988.262	384.6800	6.21	9%	$^3D^o_3$	a^3D_3	P
25990.900	384.6410	1.68	13%	$w^1G^o_4$	a^1H_5	P
26012.220	384.3257	3.70	9%	$z^1F^o_3$	a^1G_4	P
26027.178	384.1048	13.6	5%	$y^3D^o_1$	a^3F_2	L
26031.316	384.0438	4.80	6%	$y^5D^o_1$	a^5F_2	L
26039.327	383.9256	2.35	10%	$x^1G^o_4$	a^1G_4	P
26059.184	383.6330	3.29	11%	$^3D^o_2$	a^3D_2	P

Table 2. Continued

Vacuum Waveno.	λ (nm)	Trans. Prob. ($10^7 s^{-1}$)		Upper Level	Lower Level	
26073.510	383.4223	4.88	±9%	$y^5D^o_2$	a^5F_3	L
26105.995	382.9451	1.32	18%	$u^3D^o_1$	a^3D_1	P
26117.101	382.7823	11.3	5%	$y^3D^o_2$	a^3F_3	L
26130.356	382.5881	6.15	5%	$y^5D^o_3$	a^5F_4	L
26162.516	382.1178	5.54	5%	$y^3I^o_6$	b^3H_5	L
26167.670	382.0425	7.29	7%	$y^5D^o_4$	a^5P_5	L
26199.112	381.5840	11.3	5%	$y^3D^o_3$	a^3F_4	L
26234.069	381.0756	1.94	11%	$^3D^o_1$	a^3D_2	P
26262.047	380.6696	4.35	6%	$w^3H^o_5$	b^3H_5	L
26271.384	380.5343	8.60	5%	$y^3I^o_5$	b^3H_4	L
26325.535	379.7515	4.57	6%	$w^3H^o_6$	b^3H_6	L
26342.965	379.5002	1.20	7%	$y^5F^o_3$	a^5F_2	L
26392.495	378.7880	1.35	5%	$y^5F^o_2$	a^5F_1	L
26457.949	377.8509	1.17	13%	$^3D^o_2$	a^3D_3	P
26537.432	376.7192	6.50	5%	$y^5F^o_1$	a^5F_1	L
26549.079	376.5539	9.51	5%	$y^3I^o_7$	b^3H_6	L
26561.423	376.3789	5.66	5%	$y^5F^o_2$	a^5F_2	L
26600.690	375.8233	6.66	5%	$y^5F^o_3$	a^5F_3	L
26633.443	375.3611	1.22	21%	$w^5D^o_2$	a^5P_3	L
26662.749	374.9485	8.16	6%	$y^5F^o_4$	a^5F_4	L
26666.449	374.8965	1.48	9%	f^7D_5	$z^7P^o_4$	L
26680.952	374.6927	2.33	6%	f^7D_3	$z^7P^o_3$	L
26690.681	374.5561	1.16	5%	$z^5F^o_3$	a^5D_2	L
26701.077	374.4103	3.17	7%	e^7F_1	$z^7P^o_2$	L
26705.603	374.3468	6.05	5%	$^3H^o_5$	a^1H_5	L
26706.360	374.3362	2.69	6%	$y^5F^o_1$	a^5F_2	L
26742.486	373.8305	3.44	9%	$z^1I^o_6$	b^3H_5	P
26750.887	373.7131	1.42	5%	$z^5F^o_4$	a^5D_3	L
26763.831	373.5324	2.70	9%	e^7P_4	$z^7P^o_4$	P
26767.124	373.4864	9.34	5%	$y^5F^o_5$	a^5F_5	L
26784.822	373.2396	2.69	5%	$y^5S^o_2$	a^5P_2	L
26817.780	372.7809	1.91	6%	f^7D_2	$z^7P^o_3$	L
26819.148	372.7619	2.36	7%	$y^5F^o_2$	a^5F_3	L
26822.929	372.7094	1.71	14%	f^5D_3	$z^7P^o_4$	P
26824.133	372.6926	4.58	6%	e^7F_2	$z^7P^o_2$	L
26863.226	372.1503	1.94	16%	e^5G_2	$z^7P^o_2$	L
26874.549	371.9935	1.65	5%	$z^5F^o_5$	a^5D_4	L
26899.802	371.6442	3.49	10%	e^7P_3	$z^7P^o_4$	P
26936.287	371.1408	1.28	10%	$y^1D^o_2$	c^3P_1	P
26951.986	370.9246	1.67	6%	$y^5F^o_3$	a^5F_4	L
26961.628	370.7920	3.32	5%	$y^5S^o_2$	a^5P_3	L
26986.799	370.4461	1.42	9%	$y^1G^o_4$	a^3G_5	P
27011.408	370.1086	6.36	5%	e^7F_4	$z^7P^o_3$	L
27038.151	369.7426	1.94	5%	e^5G_3	$z^7P^o_3$	L
27055.520	369.5052	2.01	10%	$^1H^o_5$	a^1G_4	P
27063.178	369.4006	8.36	5%	e^7S_3	$z^7P^o_2$	L
27087.223	369.0727	2.99	10%	$^1H^o_5$	a^1H_5	P
27089.219	369.0455	1.22	11%	$^1P^o_1$	c^3P_0	P
27096.539	368.9458	3.70	5%	f^7D_4	$z^7P^o_4$	L
27121.979	368.5997	3.34	7%	e^7F_5	$z^7P^o_4$	L
27135.889	368.4108	2.97	9%	$v^3D^o_3$	a^3G_4	P
27183.701	367.7628	6.08	9%	$w^3F^o_2$	a^3G_3	P
27186.078	367.7306	2.28	13%	$^3G^o_3$	a^1D_2	P
27243.752	366.9521	2.34	9%	$w^3F^o_3$	a^3G_4	P
27348.511	365.5465	1.18	9%	$w^3P^o_2$	b^3P_2	P
27378.452	365.1467	5.84	5%	$v^3G^o_4$	a^3G_3	L
27389.234	365.0030	2.26	5%	e^7S_3	$z^7P^o_3$	L
27393.160	364.9507	3.94	9%	$w^3F^o_4$	a^3G_5	P
27405.653	364.7843	3.29	±6%	$z^5G^o_5$	a^5F_4	L
27408.805	364.7423	3.38	10%	$^1P^o_1$	c^3P_1	P
27420.857	364.5820	4.87	11%	$u^3D^o_1$	c^3P_0	P
27461.768	364.0389	3.58	5%	$v^3G^o_5$	a^3G_4	L
27477.558	363.8297	2.36	5%	$y^3H^o_4$	a^3G_3	L
27493.222	363.6224	2.20	10%	$^1F^o_3$	a^1D_2	P
27524.899	363.2039	6.75	9%	$u^3D^o_2$	c^3P_1	P
27529.262	363.1463	5.62	5%	$z^5G^o_4$	a^5F_3	L
27532.037	363.1097	2.15	9%	f^7D_5	$z^7F^o_5$	L
27601.159	362.2004	5.14	5%	$v^3G^o_3$	a^3G_3	L
27605.296	362.1461	4.46	5%	$y^3H^o_5$	a^3G_4	L
27625.837	361.8768	7.22	5%	$z^5G^o_3$	a^5F_2	L
27633.334	361.7786	7.10	9%	$u^3D^o_3$	c^3P_2	P
27677.073	361.2069	1.11	7%	e^5G_6	$z^7F^o_5$	L
27691.712	361.0159	5.90	11%	e^7F_6	$z^7F^o_6$	L
27701.686	360.8859	8.32	5%	$z^5G^o_2$	a^5F_1	L
27718.427	360.6680	8.30	5%	$y^3H^o_6$	a^3G_5	L
27727.490	360.5501	2.12	9%	f^7D_5	$z^7F^o_6$	L
27727.857	360.5453	4.67	5%	$y^3H^o_4$	a^3G_4	L
27740.436	360.3818	1.70	11%	$u^3D^o_1$	c^3P_1	P
27745.165	360.3204	2.59	5%	$v^3G^o_5$	a^3G_5	L
27750.386	360.2526	2.12	12%	e^7P_2	$z^7F^o_3$	P
27772.743	359.9626	2.33	6%	$u^3F^o_4$	a^1H_5	L
27811.321	359.4632	3.14	6%	f^7D_4	$z^7F^o_4$	L
27855.610	358.8917	2.15	11%	f^7D_1	$z^7F^o_2$	L
27858.000	358.8609	1.19	7%	e^5G_5	$z^7F^o_5$	L
27870.614	358.6985	1.66	5%	$z^5G^o_2$	a^5F_2	L
27877.390	358.6113	7.02	5%	$t^3G^o_5$	b^3H_6	L
27883.562	358.5319	1.17	5%	$z^5G^o_3$	a^5F_3	L
27886.373	358.4958	6.75	5%	$t^3G^o_4$	b^3H_5	L
27887.703	358.4787	1.56	10%	f^7D_2	$z^7F^o_3$	L
27888.692	358.4660	3.29	5%	$y^3H^o_5$	a^3G_5	L
27907.840	358.2200	2.35	10%	$^5F^o_5$	b^3H_6	P
27915.689	358.1193	10.4	8%	$z^5G^o_6$	a^5F_5	P
27961.151	357.5370	3.06	10%	$u^3D^o_2$	c^3P_2	P
27963.151	357.5114	1.60	8%	e^7F_1	$z^7F^o_1$	L
27972.739	357.3889	5.74	5%	$t^3G^o_3$	b^3H_4	L
27987.565	357.1996	2.89	6%	e^7F_5	$z^7F^o_5$	L
28002.436	357.0099	7.15	5%	$z^3G^o_5$	a^5F_4	L
28039.502	356.5379	4.29	5%	$z^3G^o_4$	a^5F_3	L
28093.584	355.8515	1.77	6%	$z^3G^o_3$	a^5F_2	L
28121.959	355.4925	14.0	5%	e^7G_6	$z^7F^o_5$	L
28131.343	355.3739	10.9	9%	$v^1G^o_4$	a^1H_5	P
28138.554	355.2828	1.74	6%	e^7F_2	$z^7F^o_2$	L
28195.599	354.5640	2.05	6%	e^7F_4	$z^7F^o_4$	L
28223.969	354.2076	9.52	5%	e^7G_4	$z^7F^o_3$	L
28231.877	354.1083	8.65	5%	e^7G_5	$z^7F^o_4$	L
28258.645	353.7729	1.33	15%	$v^3D^o_1$	b^3F_2	P
28268.018	353.6556	9.94	5%	e^7G_3	$z^7F^o_2$	L
28294.883	353.3198	8.26	5%	e^7G_2	$z^7F^o_1$	L
28296.416	353.3007	8.53	10%	e^7G_1	$z^7F^o_0$	P
28321.962	352.9820	7.75	9%	e^7G_1	$z^7F^o_1$	P
28338.234	352.7793	2.17	5%	e^7G_4	$z^7F^o_4$	L
28347.220	352.6675	5.27	5%	e^7G_2	$z^7F^o_2$	L
28348.884	352.6468	1.29	10%	$y^3P^o_2$	a^3P_2	P
28349.577	352.6381	4.13	5%	e^7G_3	$z^7F^o_3$	L
28350.730	352.6238	1.70	5%	f^5F_4	$z^7F^o_3$	L
28522.043	350.5058	1.77	10%	$^3D^o_1$	c^3P_2	P
28683.393	348.5340	1.30	11%	$w^5P^o_1$	a^5P_2	P
28757.613	347.6345	2.70	27%	i^5D_3	$z^5P^o_3$	P

(continued overleaf)

Table 2. Continued

Vacuum Waveno.	λ (nm)	Trans. Prob. ($10^7 s^{-1}$)		Upper Level	Lower Level	
28844.601	346.5861	1.19	±8%	$z^5P^o_1$	a^5D_1	P
28894.170	345.9915	2.17	9%	$^3P^o_1$	c^3P_2	P
28907.629	345.8304	2.92	10%	$x^3P^o_0$	a^3P_1	P
28961.133	345.1915	1.13	9%	$^3D^o_2$	a^5P_1	P
28974.449	345.0328	2.34	9%	$y^3P^o_1$	a^5P_1	P
29018.003	344.5149	2.34	9%	$^5D^o_3$	a^5P_2	P
29053.088	344.0989	1.24	8%	$z^5P^o_2$	a^5D_3	P
29056.320	344.0606	1.71	8%	$z^5P^o_3$	a^5D_4	P
29161.527	342.8193	1.71	10%	$^3D^o_2$	a^5P_2	P
29170.658	342.7120	5.04	9%	$^5D^o_4$	a^5P_3	P
29174.845	342.6628	1.94	9%	$y^3P^o_1$	a^5P_2	P
29188.623	342.5010	2.57	11%	$x^3F^o_3$	a^1G_4	P
29194.809	342.4285	1.61	9%	$^5D^o_3$	a^5P_3	P
29208.699	342.2656	1.38	9%	$^5D^o_2$	a^5P_1	P
29244.147	341.8507	9.89	9%	$^5D^o_0$	a^5P_1	P
29249.850	341.7841	4.01	9%	$^5D^o_1$	a^5P_1	P
29290.197	341.3133	3.23	9%	$^3D^o_3$	a^5P_2	P
29315.648	341.0169	5.07	12%	$u^3F^o_2$	a^1P_1	P
29338.957	340.7460	6.09	9%	$^3F^o_4$	a^5P_3	P
29344.642	340.6800	2.08	10%	$^3D^o_1$	a^5P_1	P
29383.828	340.2256	2.19	11%	$^3H^o_6$	b^3H_6	L
29409.093	339.9333	2.76	9%	$^5D^o_2$	a^5P_2	P
29467.004	339.2653	1.88	9%	$^3D^o_3$	a^5P_3	P
29576.342	338.0110	1.66	10%	$u^3G^o_3$	a^3G_3	P
29658.174	337.0784	2.89	9%	$u^3G^o_5$	a^3G_5	P
29669.053	336.9548	2.15	10%	$u^3G^o_4$	a^3G_4	P
29795.671	335.5228	2.59	11%	$u^3H^o_4$	b^3H_4	L
29806.051	335.4060	1.34	10%	$^3D^o_1$	b^3P_0	P
30031.619	332.8866	2.21	6%	$u^3H^o_5$	b^3H_5	L
30159.585	331.4742	7.25	5%	$u^3F^o_3$	a^3D_2	L
30228.055	330.7233	1.97	6%	$u^3H^o_6$	b^3H_6	L
30236.071	330.6356	4.84	9%	$v^5P^o_2$	a^5P_1	P
30236.210	330.6341	5.74	9%	$w^1G^o_4$	a^1G_4	P
30239.595	330.5971	4.05	9%	$v^5P^o_3$	a^5P_2	P
30367.730	329.2021	5.77	5%	$u^3F^o_4$	a^3D_3	L
30416.400	328.6753	5.99	9%	$v^5P^o_3$	a^5P_3	P
30452.184	328.2891	3.42	9%	$u^3F^o_2$	a^3D_1	P
30476.600	328.0261	4.21	5%	$x^3I^o_5$	b^3H_4	L
30613.262	326.5617	3.06	9%	$v^5P^o_2$	a^5P_3	P
30719.128	325.4362	4.24	6%	$x^3I^o_6$	b^3H_5	L
30726.329	325.3599	1.62	10%	$v^1G^o_4$	a^3D_3	P
30777.361	324.8204	1.92	9%	f^5D_3	$z^7D^o_3$	P
30815.466	324.4188	3.06	6%	f^7D_5	$z^7D^o_4$	L
30860.695	323.9433	2.95	9%	f^5D_4	$z^7D^o_4$	P
30912.846	323.3968	2.08	9%	e^7P_4	$z^7D^o_4$	P
30921.601	323.3052	4.19	5%	$x^3I^o_7$	b^3H_6	L
30948.829	323.0208	2.06	14%	e^7P_2	$z^7D^o_2$	P
30967.604	322.8249	3.72	11%	f^5D_1	$z^7D^o_2$	P
30971.953	322.7796	4.96	9%	f^5D_3	$z^7D^o_4$	P
30991.236	322.5787	11.8	6%	e^7F_6	$z^7D^o_5$	L
31027.015	322.2067	8.66	5%	f^7D_5	$z^7D^o_5$	L
31028.471	322.1916	1.22	11%	f^7D_1	$z^7D^o_1$	L
31048.819	321.9805	3.61	9%	e^7P_3	$z^7D^o_4$	P
31050.962	321.9582	4.64	5%	f^7D_4	$z^7D^o_3$	L
31072.242	321.7377	1.50	9%	f^5D_4	$z^7D^o_5$	P
31086.147	321.5938	6.19	5%	f^7D_2	$z^7D^o_2$	L
31104.294	321.4062	11.8	9%	e^7P_2	$z^7D^o_3$	P
31104.773	321.4012	8.38	5%	f^7D_3	$z^7D^o_3$	L
31124.388	321.1987	4.64	±9%	e^7P_4	$z^7D^o_5$	P
31135.605	321.0830	9.25	5%	f^7D_1	$z^7D^o_2$	L
31141.426	321.0229	1.15	6%	e^5G_5	$z^7D^o_4$	L
31188.360	320.5398	9.78	5%	e^7F_1	$z^7D^o_1$	L
31245.556	319.9530	2.23	5%	f^7D_4	$z^7D^o_4$	L
31270.994	319.6928	5.97	5%	e^7F_5	$z^7D^o_4$	L
31278.867	319.6123	1.40	5%	g^7D_4	$z^7F^o_5$	L
31306.517	319.3300	3.07	5%	e^5G_3	$z^7D^o_2$	L
31311.414	319.2801	5.01	5%	e^7F_2	$z^7D^o_1$	L
31350.507	318.8819	2.53	6%	e^5G_2	$z^7D^o_1$	L
31408.070	318.2975	1.42	15%	g^7D_3	$z^7F^o_4$	P
31422.437	318.1519	1.84	10%	$u^3D^o_2$	b^3F_3	P
31435.238	318.0224	4.42	6%	e^7F_4	$z^7D^o_3$	L
31457.101	317.8013	1.28	6%	f^7D_4	$z^7D^o_5$	L
31482.542	317.5445	1.44	6%	e^7F_5	$z^7D^o_5$	L
31523.181	317.1351	1.85	10%	$^1F^o_3$	a^1G_4	P
31572.115	316.6436	1.56	14%	$^3D^o_3$	b^3F_4	P
31629.832	316.0657	1.93	6%	e^7F_4	$z^7D^o_4$	L
31657.602	315.7885	1.61	11%	e^7S_3	$z^7D^o_2$	L
31666.111	315.7036	1.26	6%	e^7G_5	$z^7D^o_4$	L
31673.756	315.6274	6.36	11%	i^5D_3	$z^5D^o_3$	P
31797.487	314.3992	6.10	10%	i^5D_4	$z^5D^o_4$	P
31913.941	313.2519	3.39	14%	i^5D_3	$z^5D^o_4$	P
32241.790	310.0665	1.35	21%	$x^5D^o_3$	a^5F_3	L
32245.548	310.0304	1.87	13%	$x^5D^o_2$	a^5F_2	L
32249.802	309.9895	1.93	13%	$x^5D^o_1$	a^5F_1	L
32336.568	309.1577	5.53	21%	$x^5D^o_0$	a^5F_1	L
32418.729	308.3741	3.08	13%	$x^5D^o_1$	a^5F_2	L
32474.637	307.8432	1.52	10%	$u^3D^o_1$	a^3P_0	P
32503.273	307.5720	3.14	13%	$x^5D^o_2$	a^5F_3	L
32583.208	306.8174	1.11	6%	$x^3D^o_1$	a^3F_2	L
32593.085	306.7244	3.12	17%	$x^5D^o_3$	a^5F_4	L
32595.684	306.7000	1.71	17%	$^3I^o_6$	b^3H_5	L
32680.002	305.9086	1.63	11%	$y^5D^o_4$	a^5D_3	L
32697.532	305.7446	3.13	10%	$x^5D^o_4$	a^5F_5	P
32744.436	305.3066	1.53	10%	$u^3D^o_2$	a^3P_1	P
32803.111	304.7605	2.87	9%	$y^5D^o_3$	a^5D_2	L
32913.439	303.7389	2.91	9%	$y^5D^o_2$	a^5D_1	L
32975.883	303.1637	1.38	32%	$x^5F^o_1$	a^5F_1	L
32992.078	303.0149	5.04	6%	$w^3H^o_5$	a^3H_5	L
33032.263	302.6462	1.10	22%	$x^5F^o_2$	a^5F_2	L
33039.025	302.5843	3.46	5%	$y^5D^o_1$	a^5D_0	L
33041.275	302.5637	5.86	6%	$w^3H^o_6$	a^3H_6	L
33091.185	302.1073	4.70	9%	$y^5D^o_3$	a^5D_3	L
33095.939	302.0639	7.59	7%	$y^5D^o_4$	a^5D_4	L
33097.563	302.0491	1.94	9%	$y^5D^o_2$	a^5D_2	L
33196.577	301.1481	3.79	5%	$^3H^o_4$	a^3G_3	L
33217.664	300.9570	1.43	16%	$x^5F^o_4$	a^5F_4	L
33233.466	300.8138	11.1	6%	$y^5D^o_0$	a^5D_1	L
33313.095	300.0948	6.58	5%	$y^5D^o_1$	a^5D_2	L
33329.041	299.9512	1.70	22%	$x^5F^o_5$	a^5F_5	L
33363.813	299.6386	1.70	9%	$^3P^o_2$	a^3P_1	P
33385.634	299.4427	4.39	6%	$y^5D^o_2$	a^5D_3	L
33507.118	298.3570	2.94	9%	$y^5D^o_3$	a^5D_4	L
33526.433	298.1851	1.86	7%	$^3H^o_5$	a^3G_4	L
33541.260	298.0533	1.66	10%	$^3G^o_3$	a^3G_3	P
33623.579	297.3235	1.70	7%	$y^5F^o_4$	a^5D_3	L
33624.742	297.3133	1.35	7%	$y^5F^o_3$	a^5D_2	L
33659.075	297.0100	1.13	11%	$y^5F^o_2$	a^5D_1	L
33695.394	296.6898	2.96	6%	$y^5F^o_5$	a^5D_4	L

Table 2. Continued

Vacuum Waveno.	λ (nm)	Trans. Prob. ($10^7 s^{-1}$)		Upper Level	Lower Level	
33714.070	296.5255	1.28	±7%	$y^5F^o_1$	a^5D_0	L
33774.003	295.9993	5.02	7%	$^3H^o_6$	a^3G_5	L
33802.644	295.7484	1.31	18%	$^1P^o_1$	a^3P_2	P
33804.012	295.7365	1.84	7%	$y^5F^o_1$	a^5D_1	L
33843.199	295.3940	1.96	8%	$y^5F^o_2$	a^5D_2	L
33848.404	295.3486	3.64	11%	$^1F^o_3$	a^3G_3	P
33906.400	294.8434	3.32	10%	$^3G^o_4$	a^3G_4	P
33912.815	294.7876	1.83	7%	$y^5F^o_3$	a^5D_3	L
34039.510	293.6904	1.40	11%	$y^5F^o_4$	a^5D_4	L
34130.004	292.9116	15.3	14%	$t^3H^o_4$	b^3H_4	L
34173.851	292.5358	1.69	9%	$u^3H^o_4$	a^3G_3	L
34191.442	292.3853	2.97	10%	$^1H^o_5$	a^3G_5	P
34198.075	292.3286	13.9	14%	$t^3H^o_5$	b^3H_5	L
34259.726	291.8025	11.8	14%	$t^3H^o_6$	b^3H_6	L
34383.530	290.7518	1.61	9%	$u^3H^o_5$	a^3G_4	L
34449.963	290.1910	1.78	6%	g^7D_5	$z^7D^o_5$	L
34479.617	289.9415	4.68	11%	$^3D^o_1$	a^3P_2	P
34538.105	289.4504	4.83	10%	$^3P^o_2$	a^3P_2	P
34851.757	286.8454	1.45	10%	$^3P^o_1$	a^3P_2	P
35055.310	285.1797	3.37	5%	$y^5G^o_2$	a^5F_1	L
35151.701	284.3977	3.17	5%	$y^5G^o_3$	a^5F_2	L
35224.237	283.8120	1.28	5%	$y^5G^o_2$	a^5F_2	L
35294.921	283.2436	2.38	5%	$y^5G^o_4$	a^5F_3	L
35380.854	282.5556	1.32	5%	$z^5H^o_4$	a^5F_3	L
35409.425	282.3276	1.51	5%	$y^5G^o_3$	a^5F_3	L
35535.150	281.3287	3.42	5%	$y^5G^o_5$	a^5F_4	L
35614.929	280.6984	1.15	5%	$z^5H^o_5$	a^5F_4	L
35641.874	280.4862	2.40	26%	$t^3F^o_3$	a^3G_4	L
35834.279	278.9801	2.36	6%	$t^3F^o_4$	a^3G_5	L
35856.082	278.8105	5.92	5%	$y^5G^o_6$	a^5F_5	L
36099.571	276.9298	1.80	11%	$^3H^o_6$	a^3H_6	L
36122.747	276.7521	1.48	16%	$w^5D^o_4$	a^5F_4	L
36194.606	276.2027	1.76	26%	$w^5D^o_3$	a^5F_3	L
36197.839	276.1780	1.94	5%	$w^5D^o_2$	a^5F_2	L
36256.443	275.7316	2.85	5%	$w^5D^o_1$	a^5F_1	L
36269.431	275.6328	1.41	7%	$y^5P^o_2$	a^5D_1	L
36304.217	275.3687	4.00	7%	$w^5D^o_0$	a^5F_1	L
36351.027	275.0141	2.74	7%	$y^5P^o_3$	a^5D_3	L
36425.371	274.4528	2.53	5%	$w^5D^o_1$	a^5F_2	L
36431.476	274.4068	3.09	7%	$y^5P^o_1$	a^5D_0	L
36453.554	274.2406	4.70	11%	$y^5P^o_2$	a^5D_2	L
36455.564	274.2254	3.41	11%	$w^5D^o_2$	a^5F_3	L
36517.002	273.7640	1.14	10%	$^1H^o_5$	a^3H_6	P
36521.417	273.7309	7.25	7%	$y^5P^o_1$	a^5D_1	L
36545.901	273.5475	5.03	26%	$w^5D^o_3$	a^5F_4	L
36571.233	273.3581	7.10	11%	$w^5D^o_4$	a^5F_5	L
36635.028	272.8820	2.98	7%	$u^3H^o_4$	a^3H_4	L
36672.177	272.6056	5.52	5%	$^5D^o_0$	a^5F_1	L
36705.544	272.3577	5.69	9%	$y^5P^o_1$	a^5D_2	L
36741.628	272.0902	10.4	7%	$y^5P^o_2$	a^5D_3	L
36761.651	271.9420	3.20	6%	$u^3H^o_5$	a^3H_5	L
36766.527	271.9060	7.40	7%	$t^3F^o_3$	b^3F_3	L
36766.960	271.9028	14.2	5%	$y^5P^o_3$	a^5D_4	L
36774.958	271.8436	3.79	5%	$^5D^o_1$	a^5F_2	L
36908.896	270.8571	6.49	5%	$t^3F^o_4$	b^3F_4	L
36936.015	270.6582	2.69	5%	$^5D^o_2$	a^5F_3	L
36943.788	270.6013	2.28	6%	$u^3H^o_6$	a^3H_6	L
37174.572	268.9212	1.68	5%	$^5F^o_3$	a^5F_4	L
37315.413	267.9062	1.50	±5%	$^5F^o_5$	a^5F_5	L
37315.957	267.9023	1.10	9%	$x^3I^o_5$	a^3H_4	L
37449.157	266.9493	1.34	7%	$x^3I^o_6$	a^3H_5	L
37637.340	265.6145	1.63	7%	$x^3I^o_7$	a^3H_6	L
37810.240	264.3999	2.34	5%	$x^5G^o_2$	a^5F_1	L
37927.713	263.5809	2.11	5%	$x^5G^o_3$	a^5F_2	L
37979.169	263.2238	1.21	5%	$x^5G^o_2$	a^5F_2	L
38105.159	262.3534	2.13	5%	$x^5G^o_4$	a^5F_3	L
38185.438	261.8018	1.50	5%	$x^5G^o_3$	a^5F_3	L
38314.173	260.9221	4.60	13%	$^3G^o_3$	a^3G_3	P
38349.364	260.6827	2.43	5%	$x^5G^o_5$	a^5F_4	L
38456.456	259.9567	1.47	5%	$x^5G^o_4$	a^5F_4	L
38680.091	258.4536	3.15	5%	$x^5G^o_6$	a^5F_5	L
38797.860	257.6690	1.13	5%	$x^5G^o_5$	a^5F_5	L
39209.861	254.9614	2.31	10%	$x^5D^o_4$	a^5D_3	P
39265.842	254.5978	7.16	13%	$x^5D^o_3$	a^5D_2	L
39297.577	254.3922	47.1	10%	$^3I^o_5$	a^3H_4	L
39325.725	254.2101	44.8	13%	$^3I^o_6$	a^3H_5	L
39343.201	254.0972	9.60	13%	$x^5D^o_2$	a^5D_1	L
39402.083	253.7175	37.0	7%	$^3I^o_7$	a^3H_6	L
39426.439	253.5607	9.58	9%	$x^5D^o_1$	a^5D_0	L
39464.814	253.3141	2.07	12%	$^3I^o_5$	a^3H_5	L
39516.383	252.9835	3.84	9%	$x^5D^o_1$	a^5D_1	L
39524.621	252.9308	48.7	10%	$^3G^o_3$	b^3F_2	P
39527.326	252.9135	9.92	10%	$x^5D^o_2$	a^5D_2	L
39553.916	252.7435	19.3	9%	$x^5D^o_3$	a^5D_3	L
39556.545	252.7267	3.47	27%	$^3I^o_6$	a^3H_6	L
39603.150	252.4292	32.3	8%	$x^5D^o_0$	a^5D_1	L
39625.790	252.2850	21.3	9%	$x^5D^o_4$	a^5D_4	P
39676.437	251.9629	1.34	11%	$w^5G^o_2$	a^5F_1	L
39700.506	251.8102	19.3	8%	$x^5D^o_1$	a^5D_2	L
39707.452	251.7661	1.58	7%	$w^5G^o_3$	a^5F_2	L
39815.400	251.0835	12.9	8%	$x^5D^o_2$	a^5D_3	L
39861.986	250.7900	1.93	5%	$w^5G^o_4$	a^5F_3	L
39883.123	250.6571	2.04	14%	$t^3H^o_4$	b^3F_3	L
39908.011	250.5008	2.56	16%	$t^3H^o_5$	b^3F_4	L
39969.849	250.1132	6.76	13%	$x^5D^o_3$	a^5D_4	L
40043.462	249.6534	2.15	9%	$w^5G^o_5$	a^5F_4	L
40116.485	249.1989	3.25	27%	$t^3H^o_4$	b^3F_4	L
40129.915	249.1155	29.1	10%	$x^5F^o_2$	a^5D_2	L
40138.143	249.0644	34.5	10%	$x^5F^o_3$	a^5D_2	L
40152.521	248.9752	23.1	11%	$x^5F^o_1$	a^5D_0	L
40178.491	248.8143	42.0	10%	$x^5F^o_4$	a^5D_3	L
40195.890	248.7066	6.41	12%	$v^5F^o_1$	a^5F_1	P
40201.935	248.6692	1.47	10%	$v^5F^o_4$	a^5F_3	P
40242.462	248.4188	22.6	11%	$x^5F^o_1$	a^5D_1	L
40253.059	248.3534	2.09	22%	$v^5F^o_2$	a^5F_2	P
40257.306	248.3271	48.1	10%	$x^5F^o_5$	a^5D_4	L
40314.036	247.9777	17.4	10%	$x^5F^o_2$	a^5D_3	L
40318.854	247.9480	2.10	9%	$x^3P^o_2$	a^5F_2	P
40364.817	247.6657	3.05	9%	$v^5F^o_1$	a^5F_2	P
40394.866	247.4814	6.14	10%	$v^5F^o_3$	a^5F_3	P
40426.216	247.2895	13.0	10%	$x^5F^o_3$	a^5D_3	L
40426.588	247.2872	2.10	22%	$x^5F^o_1$	a^5D_2	L
40491.958	246.8880	2.40	6%	$w^5G^o_5$	a^5F_5	L
40553.230	246.5149	4.36	10%	$v^5F^o_4$	a^5F_4	P
40576.583	246.3730	1.64	10%	$x^3P^o_2$	a^5F_3	P
40594.423	246.2648	5.85	14%	$x^5F^o_4$	a^5D_4	L
40602.113	246.2181	1.10	14%	$x^5F^o_2$	a^5D_3	L
40677.845	245.7597	4.82	10%	$v^5F^o_5$	a^5F_5	P

*The last column indicates the method of measurement (lifetime L or level population P). Wavelength (column 2) is in air.

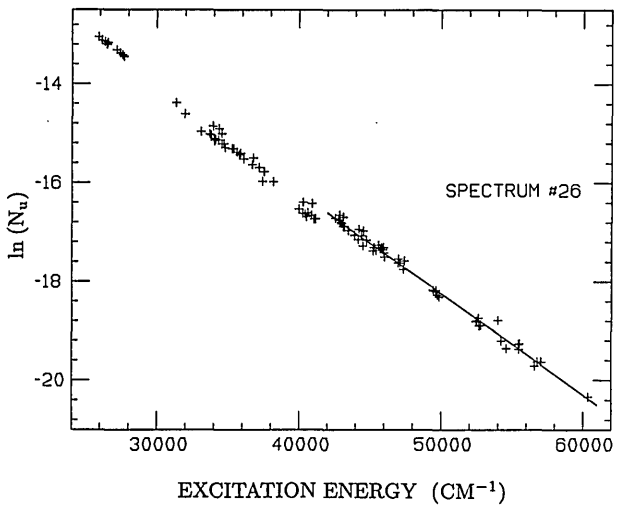

Fig. 2. Logarithm (base e) of the mean relative population per state $\bar{N}_u$ in an ICP spectrum containing a trace of $Fe(CO)_5$ as a function of level energy. The line segment is a least-squares fit to the population per state of levels above 45 000 cm^{-1}

4. TRANSITION PROBABILITIES FROM LEVEL POPULATIONS

The measured intensity $I(\lambda)$ (in photons per second) of any line of known transition probability $A(\lambda)$ is related to the population N_u per state of upper level u by

$$I(\lambda) = N_u g A(\lambda), \tag{2}$$

where g is the statistical weight of level u. In this section we use this relation in two ways. First, we find the relative population of excited levels in the ICP source by using the transition probabilities measured in Section 3. Then we interpolate between levels of known population to find the population $N_{u'}$ per state of new levels of unknown lifetime. Second, we use Eq. (2) to convert the intensity of lines from level u' into transition probabilities.

In an earlier study of Mo we found that the relative population per state of excited Mo I levels in the ICP source approximated an exponential dependence on excitation energy, as if the source were in thermal equilibrium. The Fe I populations per state of excited levels do not display such regular and easily understood behavior. It may be that Fe and Mo behave differently in the ICP source; a more likely explanation is that the extensive level information for Fe reveals irregular behavior that could not be seen with the sparse Mo population data.

When several emission lines from a level have been measured, we find a mean value of $\bar{N}_u = \Sigma_l I_{ul}/g\,\Sigma_l A_{ul}$, summed over all the emission transitions from level u seen in a IPC spectrum. This mean value $\bar{N}_u$ is shown in Fig. 2 for a broad-range spectrum (number 26-7/24/85) of an ICP source operated at relatively high power to bring up lines from high levels. The vertical scale is arbitrary: only relative populations are measured.

The population distribution in Fig. 2 shows a small upward concavity, as do all the Fe I ICP spectra that we have examined. A closer examination of individual levels shows further systematic displacements from linearity that can be seen more readily in Fig. 3, where we plot the deviation of experimental values of $\ln(N_u)$ from the straight line segment that best fits a limited region of excitation energy. The horizontal line segment shown at the top of Fig. 3 for spectrum 26 is the same line shown in Fig. 2. Levels with the shortest lifetimes (e.g., the x^5D and x^5F levels near 42 000 cm^{-1}) tend to lie lower than longer-lived levels at nearly the same excitation energy. Likewise, levels of unusually long lifetime tend to have higher populations. This dependence of population on lifetime is similar to but much smaller than that observed in the hollow-cathode source. Fortunately the deviations from a simple exponential distribution are small, and we are able to interpolate between the measured populations to estimate the populations of levels that have not been measured.

Spectrum 26 was taken with high source power, and many of the stronger lines from the lower energy levels are self-absorbed. It is advantageous to use spectra recorded at different source power levels to measure the relative population of levels in different excitation energy ranges. We use spectrum 26 only for levels with energies above 42 000 cm^{-1}, for which self-absorption is not seen on this spectrum. The populations per state fit a straight line with a rms deviation of 9% (see Fig. 3). For spectrum 30-7/25/85, used for levels between 24 000 and 42 000 cm^{-1}, the experimental populations per state fit a straight line within 8%. For spectrum 12-7/31/85, the rms deviation is 8%. Filters limited spectrum 12 to the wavenumber range 18 000–25 000 cm^{-1} in order to reduce the background noise so that the weak lines from the three lowest septet terms could be measured. Lifetimes of the septet levels are too long ($\sim 10^{-4}$ s) to be measured by the methods of Section 2. The gf values of Blackwell *et al.*[2] were used to evaluate the population of the four septet levels represented by open circles in Fig. 3.

From the linear least-squares fit to the experimental points shown in Fig. 3 one can estimate the relative population $N_{u'}$ per state of a new level u' of unknown lifetime. For at least one line λ (selected for low noise background and a good fit to the Voigt line profile) emitted from level u', we measured $I(\lambda)$ on the ICP spectrum and calculated the transition probability $A(\lambda) = I(\lambda)/gN_{u'}$, with fractional

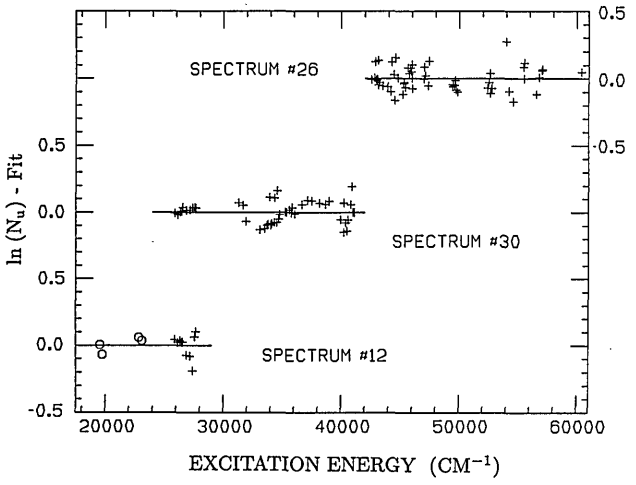

Fig. 3. Difference between $\ln(\bar{N})$ and the least-squares linear fit as a function of level energy, shown here as a horizontal line. The line segment shown for spectrum 26 is the same line as that drawn in Fig. 2; it represents a temperature of 7023 K. Populations per state of the levels represented by open circles were evaluated with gf values of Blackwell *et al.*[2]

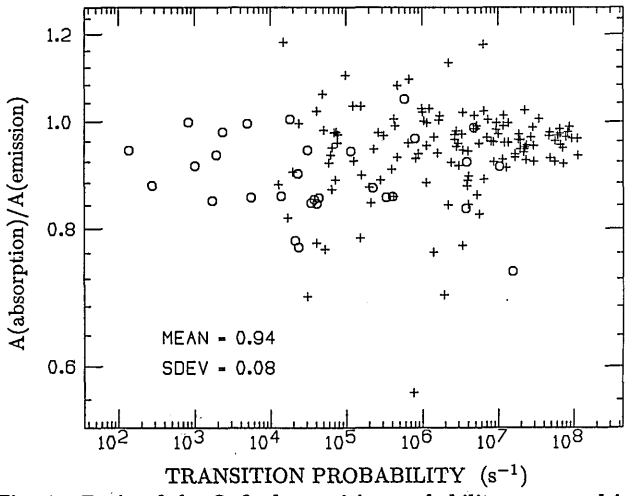

Fig. 4. Ratio of the Oxford transition probability measured in absorption to our value measured in emission for 163 ines. Pluses represent measurements by the lifetime method; circles represent measurements by interpolated level population.

uncertainty $\Delta A/A = [(\Delta I/I)^2 + (\Delta N_{u'}/N_{u'})^2]^{1/2}$. $N_{u'}$ is read from the linear fit shown in Fig. 3, and for $\Delta N_{u'}/N_{u'}$ we use the rms deviation from the linear fit to the experimental points (i.e., 9% for spectrum 26).

Additional transition probabilities $A(\lambda')$ were found from line-intensity ratios $I(\lambda')/I(\lambda)$ of other lines λ' from level u': $A(\lambda') = A(\lambda)[I(\lambda')/I(\lambda)]$ with fractional uncertainty $\Delta A'/A' = [(\Delta A/A)^2 + (\Delta I'/I')^2 + (\Delta I/I)^2]^{1/2}$. Note that complete branching fractions, required when A values are found from the level lifetime, are not needed; branching ratios $I(\lambda')/I(\lambda)$ are sufficient, and they can be measured on any spectrum. Some of the 640 transition probabilities from 104 levels measured by the population method, identified with the postscript P, appear in Table 2.

5. RESULTS AND COMPARISON WITH OTHER VALUES

Publication in this journal of all 1814 transition probabilities produced in this experiment is not feasible. In Table 2 we list values for the 478 strongest transitions that we measured. Those who need our complete results will almost certainly prefer to have them in machine-readable form. The complete list in the format of Table 2 may be obtained by BITNET request to WNW@CALTECH or by sending a 5.25 in. diskette (double sided, double density) in a reusable shipping container to W. Whaling. Include a mailing label and specify the density (360K, 1.2M) that should be used in writing the diskette, readable on an IBM or compatible microcomputer. Eventually our complete results will be deposited with the NIST Atomic Transition Probability Data Center.

We compare our transition probabilities first with the absorption oscillator strengths measured by Blackwell and his Oxford co-workers,[2] widely recognized to be the most precise values available, to justify our assumption concerning the level populations in the ICP source and to confirm the reliability of our uncertainty estimates. In Fig. 4 we plot the ratio of the Oxford transition probability (measured in absorption) to our emission value for 163 lines that are common to both experiments. For 133 lines measured by the lifetime method (represented by pluses in the figure), the mean value of the ratio A_{abs}/A_{emis} is 0.95 with a standard deviation for the sample of 0.08. For 30 lines measured by interpolation of level populations in the ICP source (the circles of Fig. 4), the corresponding ratio is 0.90 ± 0.08. We find no significant difference between the results of the two different methods. The 8% spread in the ratio A_{abs}/A_{emis} is consistent with the fractional uncertainties (in parentheses) assigned to the transition probabilities in Table 2. That this spread is no larger for the values obtained by the population method confirms our confidence in the ICP source as a useful tool for measuring transition probabilities, and the magnitude of the spread validates our uncertainty assignments.

To test the suggestion[21] of a temperature error in the Oxford measurements, we plot in Fig. 5 the ratio A_{abs}/A_{emis} as a function of the energy of the lower level in the transition. We use only stronger lines with minimum uncertainty for this test; the 66 points in Fig. 5 are all the transitions measured at Oxford and by us to which we assign an uncertainty ≤6%. As first noted by Kock *et al.*,[21] the ratio appears to be lower (by ~5%) for transitions involving levels near 20 000 cm^{-1} than it is for transitions from lower levels. However, we do not observe the exponential variation with excitation energy that is characteristic of a temperature error in the absorption furnace. Within our experimental uncertainty (5–6% for the points plotted in Fig. 5) the ratio is independent of excitation energy for levels below 14 000 cm^{-1}.

The recent critical compilation by the NIST Atomic Transition Probability Data Center[3] contains 728 of the transitions that we have measured. These include the 163 Oxford gf values, to which we have already made comparison and therefore exclude from the following discussion, plus an additional 565 values taken from many sources; many of the latter values have been adjusted or renormalized by NIST compilers to conform to the most modern and accurate standards. On average our values agree quite well with these 565 NIST values: The mean value of $\ln(A_{NIST}/A_{emis}) = 0.02 \pm 0.35$. The ±42% scatter is reasonable, since the NIST compilation includes values with an uncertainty within ±50%.

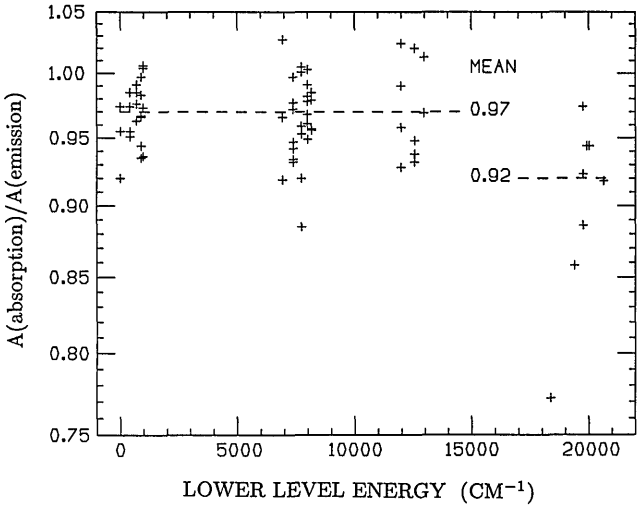

Fig. 5. Ratios from Fig. 4 plotted as a function of lower level energy. Only the strongest 66 lines with uncertainty in A_{emis} ≤ 6% are shown. The low point at 18 378 cm^{-1} was ignored for computation of the mean value shown.

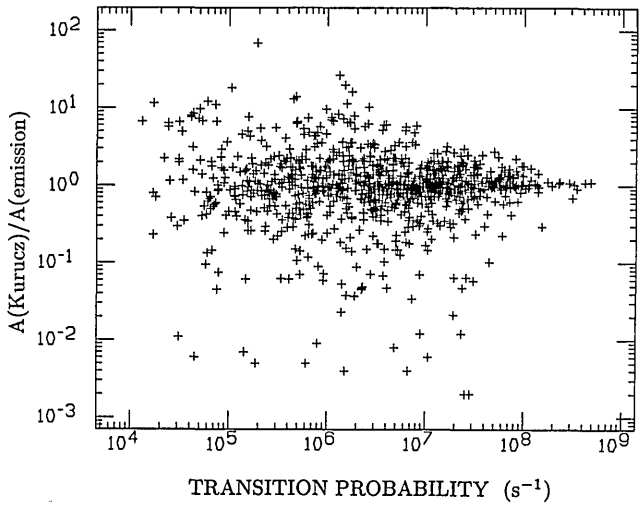

Fig. 6. Ratio of semiempirical transition probabilities computed by Kurucz[4] to our experimental values. Mean of 1117 values is 0.93. Two thirds of the theoretical values lie within a factor of 3 of the experimental values.

The recent publication by Kock *et al.*[21] of 122 Fe I transition probabilities appeared too late to be included in the NIST compilation. We have measured 110 of the transitions measured by Kock *et al.* The mean value of $\ln(A_{\text{Kock}}/A_{\text{emis}})$ is 0.02 ± 0.25.

We made extensive use of the Kurucz semiempirical transition probabilities[4] in our branching-fraction measurements, and it is of interest to find out how reliable his computed values are by comparing them with experimental values. Figure 6 shows the ratio $A_{\text{Kurucz}}/A_{\text{emis}}$ for 1117 values measured by the lifetime method; a plot of values measured from populations looks much the same. The mean value of the natural logarithm of the ratio is −0.07 ± 1.07; two thirds of the theoretical values lie within a factor of 3 of the experimental value. Since Kurucz has calculated essentially every transition between all known energy levels in Fe I, his tables are quite useful when precision of this order is adequate. We used his values in deciding when transitions outside the range of our spectra contribute negligibly to the total transition strength and also when transitions with spin change $\Delta S > 1$ may make a significant contribution.

6. Fe I LEVEL ENERGIES

Identification of lines in our FTS spectrum is based on near coincidence (within ±0.01 cm^{-1}) between the observed vacuum wave number and a predicted transition energy. The predicted line list used for this identification contains all transitions between known Fe I levels that satisfy the conditions parity change, $\delta J = 0, \pm 1$, and $\delta S = 0, \pm 1$.

Line identification on the basis of wavelength alone sets severe requirements for the level energies used in preparing the predicted line list. In addition to the obvious need for precise energies and correct J values (and if possible correct L and S values as well), there is another requirement that we have come to appreciate as we compare spectra from different sources: The level energies must be those appropriate to the spectral source used to produce the spectrum. This requirement can be satisfied only by determining the level energies from the spectrum itself, i.e., from the observed transition energies. To find level energies that meet these requirements, we carried out the following iterative process.

Step 1. Starting with the energy levels in the 1985 AEL,[5] we prepared the predicted line list, as described above, containing 12,224 lines between 8000 and 45 000 cm^{-1}.

Step 2. For a selected hollow-cathode spectrum (number 6-2/12/83), covering the range 8000–45 000 cm^{-1}, we measured all lines with a signal-to-noise ratio greater than 3, using the Kitt Peak DECOMP program to fit a Voigt profile to the observed line in order to find the line-center wave number. The observed line list contains 6280 lines, including Fe II, Ar, and Ne as well as Fe I.

Step 3. A computer search for predicted lines within 0.01 cm^{-1} of an observed line produced an identified line list of 2144 Fe I lines. In spite of the small search window, our search program assigned two different classifications to ~100 lines; i.e., two predicted lines fell within ±0.01 cm^{-1} of the observed line. The choice between the two alternative assignments could usually be made on the basis of the semiempirical gf values computed by Kurucz[4] for the two transitions. If no choice was possible, both lines were deleted. The level energies are greatly overdetermined (2144 transitions to determine 442 levels), so that a few uncertain lines could be dropped with little loss.

Step 4. The observed vacuum wave numbers in the identified line list give precise energy differences $\Delta E_{ij} = E_i - E_j$ between the level energies appropriate to our source, and the ΔE_{ij}'s can be used to find the set of most probable level energies $\{E_i\}$ by the least-squares method. We used the CLEVEL least-squares code of Palmer and Engleman[22] to solve for the energies. Their solution assigns to each observed transition $\Delta E_{ij} \pm \delta\Delta E_{ij}$ a weight proportional to $(\delta\Delta E_{ij})^{-2}$, so that a reliable estimate of the experimental uncertainty $\delta\Delta E_{ij}$ becomes an important part of the solution.

Following the analysis of Brault,[23] we take $\delta\Delta E_{ij} = (1/2)\text{FWHM}/(S/N_t)$, where FWHM is the full width at half-maximum of the line of peak amplitude S and N is the total noise amplitude. The total noise amplitude N_t has two components: In addition to the usual rms background noise N_c that one sees between lines and measures by moving several linewidths away from the line center a FTS spectrum contains another noise component N_S that is produced by variation in source brightness during the observation. N_S is proportional to the peak amplitude: $N_S = \kappa S$. Unlike N_c, which is nearly independent of wave number, N_S is present only under the line itself and can be seen and measured only after the contribution of the line from the observed spectrum is subtracted. The total noise amplitude is given by $N_t = (N_c^2 + N_S^2)^{1/2}$. The constant κ is sufficiently small (0.006 for spectrum 6-3/12/83) that the N_S is negligible except for the strongest line, where it limits S/N_t to a maximum value of ~170.

We tested our uncertainty estimate by comparing our wave numbers with those of Learner and Thorne,[24] who carefully measured 312 stronger Fe I lines as transfer wave-number standards. The average difference between our wave numbers and theirs is consistent with the uncertainty that we estimate by the method described above.

In addition to the statistical uncertainty that depends on linewidth and signal-to-noise ratio there is an uncertainty associated with the alignment factor. If the light beam entering the FTS from the source is not exactly parallel to the He–Ne laser beam that is used to monitor the mirror displacement, one must multiply the wave-number scale of the FTS by a constant factor to correct for the misalignment. We found the alignment factor $F \pm \delta F$ ($0.999\,999\,483 \pm 63$ for spectrum 6-3/12/83) by comparing the wave numbers of Ar II lines measured in our Fe + Ne + Ar spectrum with the values of Norlén.[25] For this comparison we used the 28 standard Ar II lines recommended by Learner and Thorne[24] as relatively insensitive to pressure shift.

The uncertainty $\pm\delta F$ in the alignment factor deserves some mention because it makes the largest contribution to the uncertainty in the transition energy, at least for the stronger lines that dominate the least-squares solution because of their greater weight. Although we treat F as a constant, it could depend on the energy of the upper level, because the pressure in Nolen's source was lower than that in ours; we note the effect of source pressure below in this section. Or F could vary with wave number if there is a phase error in our spectrum; Learner and Thorne[24] discuss the effect of FTS phase correction on wave number. Because of the possibility that F is dependent on variables that we ignore, we take δF to be the standard deviation of the sample of 28 independent measurements of F. δF is then a measure of our exposure to systematic error arising from the method we use to calibrate the FTS wave-number scale.

However, it should be noted that δF (and indeed the correction factor F itself) may be ignored in the transition energy $\Delta E_{ij} \pm \delta\Delta E_{ij}$ that is input to the least-squares solution and applied only to the results of the calculation, E_i, because the factor F is common to every energy term. Along with the most probable energy values E_i, the CLEVEL code also finds the uncertainty δE_i that is produced by the uncertainty in the observations. δE_i is less than 0.001 cm^{-1} for most levels and is combined with the uncertainty arising from the alignment factor $\delta E_F = (\delta F/F)E_i = (6.3 \times 10^{-8})E_i$ to obtain the total uncertainty $[(\delta E_i)^2 + (\delta E_F)^2]^{1/2}$ assigned to the level energies in Table 3.

Step 5. The level energies E_i that were determined in this least-squares solution were then used to calculate an improved version of the predicted line list, and the sequence of steps 1–4 was repeated to yield the level energies listed in Table 3, refined values for the energy of levels listed in the AEL that satisfy our requirements. The uncertainty in the last digits of the level energy appears in parentheses after the energy value. For comparison we also list the level energies from the 1985 AEL[5] The level designations follow the recommendations of Brown *et al.*[26]

A few levels are included in Table 3 even though we see only a single line from the level if (1) the line is expected to be the strongest decay channel within our spectral range on the basis of Kurucz gf values[4] and (2) Brown *et al.*[26] confirm the identification of the line in their absorption spectra.

Forty-seven levels in the AEL do not appear in Table 3. Most of the missing levels are 5p levels that decay primarily by means of IR transitions outside the 8000–45 000 cm^{-1} range of spectrum 6-3/12/83. We have seen these IR transitions on other spectra that were used for IR branching-fraction measurements, but, in the interest of presenting a set of level energies based on a single spectrum, in Table 3 we do not include the 5p-level energies that can be derived from IR transitions. The following levels were not represented on any of our spectra, even though one expects decay channels within our spectral range: $y^1H^\circ_5$ (53 722.40), $^5F^\circ_2$ (53 275.23), $z^1D^\circ_2$ (49 477.10), $r^3G^\circ_{3,4,5}$ (60 364, 60 172, 59 926 cm^{-1}). These levels were not seen in the absorption spectra of Brown *et al.*,[26] and we doubt their existence.

After we identified 2144 Fe I lines and 161 Fe II lines in spectrum 6, many unidentified lines remained. Some of these are from the neutral and ionized Ar and Ne used in the hollow-cathode source, but there are also Fe lines from unknown Fe I levels. We searched for new levels by adding and subtracting the energy ΔE_u of unclassified transitions to our known energy levels E_i of odd (or even) parity. The set $\{E_i \pm \Delta E_u\}_{iu}$ contains possible values for an unknown even-parity energy level involved in the transition of energy ΔE_u. A cluster of close values in this set, where all partner levels satisfy the δJ selection rule, suggests a possible even- (or odd-) parity level. Additional tests and details of the search procedure are described in Ref. 1. The following levels that do not appear in the 1985 AEL[5] were identified in this way:

$E = 43\,460.117$ cm^{-1}, $J = 5$, odd parity; $E = 43\,442.699$ cm^{-1}, $J = 4$, odd parity. Brown *et al.*[26] also saw these levels in absorption and labeled them $z^5I^\circ_5$ and $z^5I^\circ_4$, respectively.

$E = 49\,477.124$ cm^{-1}, $J = 3$, odd parity, probably $S = 0$ because strong transitions are to singlet levels. The AEL lists a level nearby at 49 477.10 cm^{-1}, but its designation $z^1D^\circ_2$ is wrong. We believe that this level should be labeled $3d^6(a^3F)4s4p(^3P^\circ)^1F^\circ_3$ because a singlet F level is expected in this neighborhood, and the level labeled $^1F_3$ in the AEL at 49 227.12 cm^{-1} is one of those for which we see no evidence.

$E = 53\,852.110$ cm^{-1}, $J = 4$, odd parity. We believe that this is the correct J assignment for the level designated $^5G^\circ_3$ in the AEL at 53 852.108 cm^{-1}.

$E = 24\,574.650$ cm^{-1}, $J = 4$, even parity, $a\,^1G_4$ in the AEL. Many emission lines to this level appear in our spectrum: 8 lines (including the strongest) are from singlet upper levels, 16 are from triplet upper levels, 9 are from quintet levels, and 1 is from a level of unknown spin. The quintet partners would lead us to classify this as a triplet level, but Johansson[27] advises that the $\delta S = 2$ transitions reflect spin impurity in the high odd partners. We have not seen $\delta S = 2$ transitions to other levels, but a thorough search with a $\delta S = 2$ predicted line list has not been made.

The level energies in Table 3 are notable in two respects: They have greater precision than any other comprehensive set now available, and they constitute a self-consistent set because all level energies were derived from a single spectrum. A transition energy ΔE, obtained from the difference between level energies in Table 3, is far more precise than either level energy alone, because the systematic uncertainty in ΔE is only 6.3×10^{-8} ΔE. However, we em-

Table 3. Fe I Level Energy*

Level	Energy (cm^{-1})	(±)	NIST Lines
a $^5D_4$	0.0000(00)	.000	31
a $^5D_3$	415.9333(02)	.932	38
a $^5D_2$	704.0061(02)	.004	46
a $^5D_1$	888.1313(03)	.129	33
a $^5D_0$	978.0730(03)	.072	14
a $^5F_5$	6928.2673(05)	.266	47
a $^5F_4$	7376.7630(05)	.760	59
a $^5F_3$	7728.0584(05)	.056	66
a $^5F_2$	7985.7832(06)	.780	62
a $^5F_1$	8154.7115(06)	.710	44
a $^3F_4$	11976.2370(08)	.234	41
a $^3F_3$	12560.9325(08)	.930	39
a $^3F_2$	12968.5518(09)	.549	26
a $^5P_3$	17550.1783(11)	.175	45
a $^5P_2$	17726.9851(11)	.981	55
a $^5P_1$	17927.3805(12)	.376	36
a $^3P_2$	18378.1825(12)	.181	38
z $^7D^o_5$	19350.8906(13)	.892	13
a $^3H_6$	19390.1644(13)	.164	24
a $^3P_1$	19552.4752(13)	.473	25
z $^7D^o_4$	19562.4381(13)	.440	19
a $^3H_5$	19621.0050(13)	.005	36
z $^7D^o_3$	19757.0298(13)	.033	16
a $^3H_4$	19788.2482(13)	.245	30
z $^7D^o_2$	19912.4942(13)	.494	15
z $^7D^o_1$	20019.6345(14)	.635	13
a $^3P_0$	20037.8142(15)	.813	9
b $^3F_4$	20641.1079(14)	.109	38
b $^3F_3$	20874.4782(14)	.484	28
b $^3F_2$	21038.9835(14)	.985	19
a $^3G_5$	21715.7303(14)	.730	39
a $^3G_4$	21999.1274(14)	.127	42
a $^3G_3$	22249.4265(15)	.428	35
z $^7F^o_6$	22650.4144(15)	.421	7
b $^3P_2$	22838.3197(15)	.318	33
z $^7F^o_5$	22845.8667(15)	.868	15
b $^3P_1$	22946.8120(15)	.808	31
z $^7F^o_4$	22996.6713(15)	.676	20
b $^3P_0$	23051.7472(16)	.742	11
z $^7F^o_3$	23110.9362(15)	.937	17
z $^7F^o_2$	23192.4960(15)	.497	18
z $^7F^o_1$	23244.8352(15)	.834	11
z $^7F^o_0$	23270.3816(16)	.374	3
z $^7P^o_4$	23711.4536(15)	.457	21
b $^3G_5$	23783.6154(16)	.614	23
b $^3G_4$	24118.8141(16)	.814	31
z $^7P^o_3$	24180.8607(16)	.864	21
c $^3P_2$	24335.7631(16)	.759	29
b $^3G_3$	24338.7626(17)	.762	17
z $^7P^o_2$	24506.9160(16)	.919	14
a $^1G_4$	24574.6497(16)	.650	33
c $^3P_1$	24772.0147(18)	.017	17
c $^3P_0$	25091.5948(23)	.597	6
z $^5D^o_4$	25899.9860(17)	.987	24
b $^3H_6$	26105.9041(17)	.904	17
z $^5D^o_3$	26140.1762(17)	.177	28
a $^3D_3$	26224.9648(18)	.966	23
z $^5D^o_2$	26339.6933(17)	.691	21
b $^3H_5$	26351.0361(17)	.039	17
a $^3D_1$	26406.4606(20)	.470	9
z $^5D^o_1$	26479.3764(17)	.376	14
z $^5D^o_0$	26550.4748(17)	.476	7
a $^3D_2$	26623.7300(21)	.730	20
b $^3H_4$	26627.6048(18)	.604	18
z $^5F^o_5$	26874.5464(17)	.549	17
z $^5F^o_4$	27166.8170(17)	.819	21
z $^5F^o_3$	27394.6869(17)	.688	21
a $^1P_1$	27542.9991(21)	.004	10
z $^5F^o_2$	27559.5797(18)	.581	19
z $^5F^o_1$	27666.3441(18)	.346	17
a $^1D_2$	28604.6070(20)	.606	12
a $^1H_5$	28819.9513(19)	.946	18
z $^5P^o_3$	29056.3216(18)	.321	20
a $^1I_6$	29313.0024(20)	.003	5
b $^3D_1$	29320.0275(53)	.028	3
b $^3D_2$	29356.7324(32)	.740	8
b $^3D_3$	29371.8062(30)	.811	5
z $^5P^o_2$	29469.0211(19)	.020	21
z $^5P^o_1$	29732.7325(19)	.733	14
b $^1G_4$	29798.9303(26)	.933	6
z $^3F^o_4$	31307.2425(20)	.243	12
z $^3D^o_3$	31322.6094(20)	.611	14
z $^3D^o_2$	31686.3476(20)	.346	11
z $^3F^o_3$	31805.0674(20)	.067	13
z $^3D^o_1$	31937.3212(21)	.316	11
z $^3F^o_2$	32133.9868(21)	.986	11
c $^3F_4$	32873.6264(23)	.619	13
y $^5D^o_4$	33095.9368(21)	.937	15
c $^3F_3$	33412.7109(24)	.713	11
y $^5D^o_3$	33507.1187(21)	.120	19
y $^5F^o_5$	33695.3935(22)	.394	13
c $^3F_2$	33765.3000(27)	.304	7
y $^5D^o_2$	33801.5684(22)	.567	18
z $^3P^o_2$	33946.9286(22)	.929	17
y $^5D^o_1$	34017.0989(22)	.098	15
y $^5F^o_4$	34039.5118(22)	.513	18
y $^5D^o_0$	34121.5976(22)	.58	7
y $^5F^o_3$	34328.7488(22)	.749	24
z $^3P^o_1$	34362.8683(22)	.871	15
y $^5F^o_2$	34547.2057(22)	.206	19
z $^3P^o_0$	34555.5934(22)	.60	5
b $^1D_2$	34636.7762(70)	.78	1
y $^5F^o_1$	34692.1437(22)	.144	12
z $^5G^o_5$	34782.4168(22)	.416	11
z $^5G^o_6$	34843.9515(22)	.94	3
z $^5G^o_4$	35257.3206(22)	.319	17
z $^3G^o_5$	35379.2036(23)	.206	15
z $^5G^o_3$	35611.6205(23)	.619	13
z $^3G^o_4$	35767.5604(23)	.561	20
z $^5G^o_2$	35856.3971(23)	.400	12
z $^3G^o_3$	36079.3679(23)	.366	20
y $^3F^o_4$	36686.1719(23)	.164	26
y $^5P^o_3$	36766.9615(24)	.962	13
y $^5P^o_2$	37157.5635(24)	.557	10
y $^3F^o_3$	37162.7425(24)	.740	22
y $^5P^o_1$	37409.5493(25)	.542	7
y $^3F^o_2$	37521.1567(24)	.157	15
y $^3D^o_3$	38175.3499(24)	.350	21
y $^3D^o_2$	38678.0346(25)	.032	18
y $^3D^o_1$	38995.7302(25)	.730	14
x $^5D^o_4$	39625.7983(25)	.800	9
x $^5D^o_3$	39969.8482(25)	.844	7
y $^7P^o_2$	40052.0345(28)	.030	3
y $^7P^o_3$	40207.0895(26)	.086	8
x $^5D^o_2$	40231.3317(26)	.332	6
x $^5F^o_5$	40257.3085(26)	.307	6
x $^5D^o_1$	40404.5131(26)	.506	5
y $^7P^o_4$	40421.9368(27)	.85	4
x $^5D^o_0$	40491.2793(27)	.274	2
x $^5F^o_4$	40594.4270(26)	.429	5
x $^5F^o_3$	40842.1492(26)	.151	7
z $^5S^o_2$	40894.9859(26)	.986	8
x $^5F^o_2$	41018.0462(26)	.050	5
x $^5F^o_1$	41130.5942(27)	.627	3
x $^5P^o_3$	42532.7374(27)	.736	8
y $^5G^o_6$	42784.3489(28)	.35	1
e $^7D_5$	42815.8506(27)	.858	6
x $^5P^o_2$	42859.7729(27)	.770	8
y $^5G^o_5$	42911.9125(28)	.908	2
z $^5H^o_5$	42991.6920(28)	.62	3
y $^5G^o_4$	43022.9798(28)	.975	3
x $^5P^o_1$	43079.0202(29)	.026	6
z $^5H^o_4$	43108.9125(28)	.90	4
y $^5G^o_3$	43137.4834(28)	.479	4
e $^7D_4$	43163.3209(27)	.327	8
y $^5G^o_2$	43210.0208(28)	.021	3
z $^5H^o_3$	43325.9594(28)	.958	5
e $^7D_3$	43434.6237(28)	.629	9
z $^5I^o_4$	43442.6999(29)		5
z $^5I^o_5$	43460.1170(48)		2
w $^5D^o_4$	43499.5013(28)	.496	4
e $^7D_2$	43633.5288(28)	.534	7
e $^7D_1$	43763.9765(28)	.980	6
w $^5D^o_3$	43922.6639(28)	.664	10
v $^5D^o_4$	44022.5204(28)	.535	7
v $^5D^o_3$	44166.1994(28)	.203	7
w $^5D^o_2$	44183.6228(28)	.620	13
w $^5F^o_5$	44243.6800(29)	.673	3
w $^5F^o_2$	44285.4513(29)	.443	6
w $^5F^o_1$	44378.3365(29)	.38?	3
w $^5D^o_1$	44411.1549(29)	.151	7
w $^5F^o_4$	44415.0688(28)	.070	6
w $^5D^o_0$	44458.9284(30)	.92	2

Table 3. Continued

Level	Energy (cm^{-1})	(±)	NIST Lines
y $^5S^o_2$	44511.8064(28)	.806	7
w $^5F^o_3$	44551.3333(29)	.330	6
v $^5D^o_2$	44664.0726(29)	.068	5
e $^5D_4$	44677.0017(28)	.004	6
v $^5D^o_1$	44760.7409(29)	.75	3
v $^5D^o_0$	44826.8940(30)	.88	1
e $^5D_3$	45061.3245(29)	.327	8
x $^3D^o_3$	45220.6752(29)	.676	8
x $^3D^o_2$	45281.8273(29)	.831	12
y $^3G^o_5$	45294.8414(29)	.846	9
e $^5D_2$	45333.8716(29)	.874	9
y $^3G^o_4$	45428.3978(29)	.397	12
e $^5D_1$	45509.1481(29)	.150	7
x $^3D^o_1$	45551.7607(29)	.763	8
y $^3G^o_3$	45562.9699(29)	.970	11
e $^5D_0$	45595.0850(29)	.08	2
x $^5G^o_6$	45608.3581(30)	.31?	2
x $^5G^o_5$	45726.1276(30)	.117	2
x $^5G^o_4$	45833.2181(30)	.20	4
x $^5G^o_3$	45913.4965(30)	.488	3
x $^5G^o_2$	45964.9522(30)	.959	3
z $^3I^o_7$	45978.0024(30)	.00?	2
z $^3I^o_6$	46026.9668(30)	.94	3
z $^3I^o_5$	46135.8123(30)	.88	4
w $^5P^o_3$	46137.0922(30)	.10	3
w $^5P^o_2$	46313.5361(32)	.57	4
w $^5P^o_1$	46410.3780(36)	.40	1
z $^3S^o_1$	46600.8139(32)	.814	6
y $^3P^o_0$	46672.5360(33)	.527	3
u $^5D^o_4$	46720.8368(30)	.836	9
y $^3P^o_2$	46727.0675(30)	.068	9
u $^5D^o_3$	46744.9882(30)	.988	9
u $^3D^o_2$	46888.5124(30)	.510	12
x $^3F^o_4$	46889.1363(30)	.143	9
y $^3P^o_1$	46901.8291(30)	.820	10
z $^3H^o_6$	46982.3149(30)	.34	5
e $^5F_5$	47005.5013(30)	.508	8
z $^3H^o_5$	47008.3655(30)	.366	13
w $^3D^o_3$	47017.1823(30)	.188	9
x $^3F^o_3$	47092.7060(30)	.707	12
z $^3H^o_4$	47106.4787(30)	.477	16
w $^3D^o_2$	47136.0792(30)	.072	10
u $^5D^o_0$	47171.5276(31)	.48?	1
u $^5D^o_1$	47177.2302(30)	.225	7
x $^3F^o_2$	47197.0051(30)	.014	14
w $^3D^o_1$	47272.0229(30)	.016	9
w $^5G^o_6$	47363.3703(30)	.369	4
e $^5F_4$	47377.9491(30)	.962	13
$^1D^o_2$	47419.6829(31)	.674	9
w $^5G^o_5$	47420.2250(31)	.229	5
z $^1G^o_4$	47452.7106(30)	.716	9
y $^3S^o_1$	47555.6044(31)	.598	9
w $^5G^o_4$	47590.0437(31)	.047	8
v $^5F^o_5$	47606.1118(32)	.094	2
w $^5G^o_3$	47693.2354(31)	.227	7
e $^5F_3$	47755.5311(30)	.539	14
x $^3G^o_4$	47812.1132(31)	.118	12
w $^5G^o_2$	47831.1487(31)	.150	5
x $^3G^o_3$	47834.2152(32)	.218	7
x $^3G^o_5$	47834.5456(31)	.542	12
v $^5F^o_4$	47929.9933(31)	.999	6
e $^3F_4$	47960.9366(31)	.941	14
v $^5P^o_3$	47966.5793(31)	.59	2
e $^5F_2$	48036.6664(31)	.666	14
v $^5F^o_3$	48122.9249(32)	.928	5
v $^5P^o_2$	48163.4445(36)	.438	5
e $^5F_1$	48221.3162(32)	.314	9
y $^5H^o_5$	48231.2742(31)	.270	8
v $^5F^o_2$	48238.8432(31)	.844	13
x $^3P^o_2$	48304.6376(31)	.638	11
v $^5F^o_1$	48350.6012(32)	.601	3
y $^5H^o_4$	48361.8749(31)	.878	9
z $^1H^o_5$	48382.5961(31)	.597	7
x $^3P^o_0$	48460.1060(33)	.098	5
y $^5H^o_3$	48475.6797(32)	.668	6
x $^3P^o_1$	48516.1336(32)	.135	14
e $^3F_3$	48531.8621(31)	.864	9
y $^1G^o_4$	48702.5291(31)	.526	8
e $^3F_2$	48928.3834(32)	.389	8
w $^3F^o_4$	49108.8903(31)	.890	9
v $^3D^o_3$	49135.0166(32)	.022	9
v $^3D^o_2$	49242.6149(32)	.593	8
w $^3F^o_3$	49242.8798(32)	.881	10
v $^3D^o_1$	49297.6282(34)	.620	4
w $^3F^o_2$	49433.1275(32)	.121	5
y $^3H^o_6$	49434.1569(32)	.156	4
v $^3G^o_5$	49460.8953(31)	.890	9
$^1F^o_3$	49477.1226(32)	.10	7
y $^3H^o_5$	49604.4226(32)	.415	6
v $^3G^o_4$	49627.8787(32)	.877	11
y $^3H^o_4$	49726.9845(32)	.977	8
v $^3G^o_3$	49850.5847(32)	.581	7
w $^3P^o_0$	49951.3397(37)	.341	3
w $^3P^o_1$	50043.2072(34)	.205	8
w $^3P^o_2$	50186.8283(32)	.830	8
e $^7F_6$	50342.1264(32)	.14	3
f $^7D_5$	50377.9043(32)	.913	6
f $^5D_4$	50423.1330(32)	.136	11
e $^7P_4$	50475.2833(32)	.287	7
e $^5G_6$	50522.9396(32)	.946	5
f $^5D_3$	50534.3900(32)	.391	7
z $^1F^o_3$	50586.8699(33)	.874	6
e $^7P_3$	50611.2565(33)	.260	9
x $^1G^o_4$	50613.9767(33)	.972	7
e $^7G_7$	50651.6290(33)	.72?	1
f $^5D_2$	50698.6159(33)	.624	9
e $^5G_5$	50703.8651(32)	.866	10
f $^7D_4$	50807.9925(32)	.991	8
e $^7F_5$	50833.4321(32)	.428	6
e $^7P_2$	50861.3238(33)	.321	4
f $^7D_3$	50861.8124(35)	.816	6
f $^5D_1$	50880.0978(35)	.098	7
e $^7G_6$	50967.8260(33)	.826	4
e $^5G_4$	50979.5741(33)	.578	8
f $^5D_0$	50981.0019(42)	.98	4
f $^7D_2$	50998.6408(33)	.641	10
u $^5F^o_5$	51016.6581(40)	.660	1
x $^3H^o_6$	51023.1572(33)	.152	4
f $^7D_1$	51048.1002(34)	.113	5
x $^3H^o_5$	51068.7103(33)	.710	9
t $^5D^o_4$	51076.6216(37)	.622	1
f $^5F_5$	51103.1870(33)	.187	5
e $^7F_3$	51148.8411(44)	.859	2
e $^5S_2$	51148.9040(43)	.883	2
e $^7F_4$	51192.2686(33)	.270	5
v $^3F^o_2$	51201.2828(35)	.284	6
e $^7F_1$	51207.9943(34)	.991	6
e $^5G_3$	51219.0113(33)	.017	9
e $^7G_5$	51228.5487(33)	.555	7
e $^3D_3$	51294.2160(33)	.222	6
v $^3F^o_4$	51304.5994(33)	.603	11
e $^7F_2$	51331.0486(34)	.044	6
e $^7G_4$	51334.9052(33)	.909	8
g $^5D_4$	51350.4883(33)	.491	14
t $^5D^o_3$	51361.3872(55)	.390	4
v $^3F^o_3$	51365.3046(34)	.308	6
e $^5G_2$	51370.1413(34)	.130	6
u $^3G^o_5$	51373.9040(33)	.909	7
u $^5F^o_4$	51381.4511(32)	.460	3
x $^3H^o_4$	51409.1209(36)	.117	5
e $^7G_3$	51460.5140(33)	.516	6
f $^5F_4$	51461.6664(33)	.672	7
e $^7G_2$	51539.7171(33)	.712	5
e $^7G_1$	51566.7978(34)	.82	3
e $^7S_3$	51570.0942(33)	.084	5
f $^5F_3$	51604.0999(34)	.102	7
$^1H^o_5$	51630.1714(34)	.172	8
u $^3G^o_4$	51668.1812(33)	.189	9
f $^5F_2$	51705.0108(36)	.007	4
y $^1D^o_2$	51708.3018(35)	.309	7
e $^3D_2$	51739.9155(33)	.920	13
f $^5F_1$	51754.4933(42)	.490	4
x $^1D^o_2$	51762.0726(37)	.067	7
g $^5D_3$	51770.5537(34)	.554	14
u $^3G^o_3$	51825.7689(33)	.773	9
u $^5F^o_2$	51827.4078(50)	.413	1
e $^5P_3$	51837.2338(34)	.24	8
u $^3D^o_3$	51969.0956(34)	.079	5
e $^5P_1$	52019.6644(40)	.67	5
e $^3D_1$	52039.8869(34)	.886	4
g $^5D_2$	52049.8188(36)	.814	12
e $^5P_2$	52067.4642(34)	.460	8
$^1P^o_1$	52180.8158(36)	.804	4

(continued overleaf)

Table 3. Continued

Level	Energy (cm^{-1})	(±)	NIST	Lines
t $^3D^o_3$	52213.2258(34)	.226		5
g $^5D_1$	52214.3378(36)	.336		9
g $^5D_0$	52257.3372(50)	.33		3
u $^3D^o_2$	52296.9131(35)	.899		7
w $^3H^o_6$	52431.4388(34)	.418		3
u $^3D^o_1$	52512.4511(39)	.445		6
y $^3I^o_6$	52513.5523(34)	.549		5
w $^3H^o_5$	52613.0827(34)	.084		5
y $^3I^o_7$	52654.9835(34)	.00?		2
t $^3D^o_2$	52682.9133(37)	.915		5
w $^3H^o_4$	52768.7353(34)	.721		4
t $^3D^o_1$	52857.7998(38)	.790		7
y $^3I^o_5$	52898.9891(35)	.971		3
v $^3P^o_2$	52916.2874(36)	.292		6
$^5F^o_4$	52953.6235(43)	.625		3
g $^5F_5$	53061.3100(34)	.24		4
z $^1I^o_6$	53093.5226(34)	.521		3
h $^5D_4$	53155.1386(34)	.09		6
f $^5P_3$	53160.5863(34)	.49		4
f $^5G_6$	53169.1380(34)	.17		2
v $^3P^o_1$	53229.9333(38)	.942		7
e $^5H_7$	53275.1747(34)	.16?		1
f $^5G_5$	53281.6819(34)	.70		5
$^3F^o_4$	53328.8273(54)	.827		4
e $^5H_6$	53352.9803(34)	.98?		1
$^3F^o_3$	53357.5057(44)	.508		3
g $^5F_4$	53393.6677(35)	.68		9
h $^5D_3$	53545.8252(35)	.847		7
f $^5P_2$	53568.7461(36)	.68		4
$^5D^o_4$	53610.4102(37)	.414		4
$^5F^o_3$	53661.0699(45)	.09		4
$^5F^o_3$	53733.5857(64)	.583		3
e $^3G_5$	53739.4300(34)	.433		5
f $^3D_3$	53747.4935(35)	.51		6
$^3F^o_2$	53749.4045(57)	.405		3
x $^1F^o_3$	53763.2731(36)	.272		5
f $^5G_4$	53768.9723(35)	.969		8
g $^7D_5$	53800.8544(46)	.841		3
x $^3S^o_1$	53808.3530(42)	.353		6
g $^5F_3$	53830.9687(40)	.973		6
$^3D^o_3$	53837.8513(51)	.847		5
e $^3H_6$	53840.6131(34)	.64?		2
$^5G^o_4$	53852.1095(40)	.108		3
e $^5H_5$	53874.2496(34)	.26?		2
$^5D^o_3$	53891.5211(37)	.520		3
f $^5P_1$	53925.1929(43)	.22		2
h $^5D_2$	53966.6537(37)	.68		5
t $^3G^o_5$	53983.2938(35)	.284		1
t $^5P^o_3$	54004.7131(38)	.78		1
$^5F^o_5$	54013.7442(35)	.747		3
$^3G^o_4$	54017.5789(60)	.573		3
e $^3G_4$	54066.5109(35)	.53		6
f $^3D_2$	54066.7668(37)	.758		8
t $^5P^o_2$	54112.2259(38)	.218		3
g $^7D_4$	54124.7362(52)	.724		3
h $^5D_1$	54132.5451(45)	.550		3
f $^5G_3$	54161.1306(36)	.132		6
e $^5H_4$	54237.1471(45)	.16		1
t $^3G^o_4$	54237.4088(36)	.415		6
g $^5F_2$	54257.4914(42)	.505		5
e $^3H_5$	54266.7069(35)	.72?		3
t $^5P^o_1$	54271.0594(40)	.057		3
$^5D^o_4$	54301.3356(38)	.334		3
$^3G^o_3$	54357.3991(52)	.398		3
f $^5G_2$	54375.6713(36)	.68		4
e $^3G_3$	54379.3787(35)	.40		4
g $^5F_1$	54386.1798(47)	.189		3
g $^7D_3$	54404.7414(59)	.765		1
f $^3D_1$	54449.3414(47)	.29		4
e $^5H_3$	54490.9919(35)	.04		1
e $^3H_4$	54555.4122(35)	.41?		4
t $^3G^o_3$	54600.3437(37)	.346		7
g $^7D_2$	54611.7101(13)	.691		2
f $^3F_4$	54683.3156(36)	.35		4
w $^1G^o_4$	54810.8591(35)	.841		4
e $^3P_2$	54879.6751(38)	.68		2
f $^3F_3$	55124.9326(37)	.93		3
e $^3P_1$	55376.0839(45)	.08		2
f $^3F_2$	55378.7899(45)	.80		2
s $^3G^o_5$	55429.8124(36)	.815		5
$^3H^o_4$	55446.0034(37)	.000		3
$^3H^o_6$	55489.7333(36)	.77		3
$^3H^o_5$	55525.5554(36)	.54		6
e $^3P_0$	55726.5239(41)	.50?		1
w $^1D^o_2$	55754.2280(38)	.239		4
s $^3G^o_3$	55790.6860(39)	.673		3
s $^3G^o_4$	55905.5278(38)	.538		5
$^1H^o_5$	55907.1731(37)	.171		7
$^1F^o_3$	56097.8303(40)	.829		4
u $^3H^o_6$	56333.9550(37)	.957		3
u $^3H^o_5$	56382.6558(37)	.662		5
u $^3H^o_4$	56423.2761(37)	.279		6
u $^3F^o_4$	56592.6944(39)	.699		4
u $^3F^o_3$	56783.3149(42)	.317		2
u $^3F^o_2$	56858.6461(45)	.659		2
v $^1G^o_4$	56951.2942(37)	.286		3
x $^3I^o_7$	57027.5049(37)	.52?		2
x $^3I^o_6$	57070.1637(37)	.21		3
x $^3I^o_5$	57104.2045(38)	.22		4
t $^3F^o_4$	57550.0047(39)	.000		3
t $^3F^o_3$	57641.0056(50)	.000		4
i $^5D_4$	57697.4863(48)	.55		4
t $^3F^o_2$	57708.7420(76)	.747		2
i $^5D_3$	57813.9325(70)	.940		1
i $^5D_2$	57974.1340(63)	.129		2
g $^5G_6$	58001.9311(40)	.84		3
g $^5G_5$	58271.4578(53)	.46?		1
g $^5G_4$	58520.1739(84)	.14?		2
g $^5G_3$	58710.0353(45)	.05?		4
$^3I^o_7$	58792.2473(41)			1
$^3I^o_6$	58946.7297(41)			2
$^3I^o_5$	59085.8249(40)			2
t $^3H^o_6$	60365.6309(40)	.70		2
t $^3H^o_5$	60549.1110(47)	.18		2
$^3G^o_3$	60563.6041(44)	.61		2
t $^3H^o_4$	60757.6029(53)	.68		2

*The column headed NIST shows decimal digits of the energy given in Ref. 5. Last column shows the number of measured transitions involving the level. The uncertainty in the last digit(s) appears in parentheses.

phasize that these level energies apply to a particular hollow-cathode source (8 mm in diameter by 30 mm long, 0.85 A at 250 V, 2.5 Torr Ne + 0.6 Torr Ar). By the same method we measured level energies in the inductively coupled Ar plasma source at a pressure of 600 Torr. Fe I level energies in the ICP source are shifted by as much as ±0.02 cm^{-1}, and in both directions, from those in Table 3.

We compared our level energies with those in the 1985 AEL of Sugar and Corliss[5] and with the recent measurements of absorption spectra by Brown *et al.*[26] The third column of Table 3 shows the decimal digits of the level energy from the AEL; for 31 levels (excluding those levels noted in the AEL by a question mark or with only one or two digits after the decimal) we differ from the AEL value by ≥0.010 cm^{-1}. Our values differ from the level energies measured by Brown *et al.* by more than 0.02 cm^{-1} for six levels. We have carefully reexamined and confirmed the experimental evidence for those values that are in disagreement.

ACKNOWLEDGMENTS

This research was supported in part by National Science Foundation grants AST 87-13904 and AST 88-21051. W. Whaling was a guest observer at the National Solar Observatory (Kitt Peak) during this research. The ICP used in this work was first brought to the National Solar Observatory by Lynda M. Faires of Los Alamos National Laboratory to investigate the potential of an ICP FTS for analytical chemistry, and we are grateful for her assistance in the operation of the source for the acquisition of the present data. We are also grateful to Rolf Engleman, formerly of that laboratory, who has been responsible for a number of improvements in our use of both the hollow-

cathode source and the ICP source (especially with respect to the use of carbonyl and halide vapors of several metals). M. J. Seaton of University College, London, kindly provided unpublished He gf values that were used to calibrate the IR response of the FTS. We are indebted to R. L. Kurucz of the Center for Astrophysics for generously supplying millions of semiempirical gf values. Finally, we thank S. E. Johansson for valued criticism of our Fe I level energies.

The National Solar Observatory, National Optical Astronomy Observatory, is operated by the Association of Universities for Research in Astronomy, Inc., under a cooperative agreement with the National Science Foundation.

REFERENCES

1. W. Whaling and J. W. Brault, "Comprehensive transition probabilities in Mo I," Phys. Scr. **38,** 707–718 (1988).
2. D. E. Blackwell, A. D. Petford, and G. J. Simmons, "Measurements of relative oscillator strengths for Fe I," Mon. Not. R. Astron. Soc. **201,** 595–602 (1982), and references therein.
3. J. R. Fuhr, G. A. Martin, and W. L. Wiese, "Atomic transition probabilities: Fe through Ni," J. Phys. Chem. Ref. Data **17,** Suppl. 4 (1988).
4. R. L. Kurucz, "Semi-empirical calculation of gf-values for the iron group," Trans. Int. Astron. Union B **20,** 168–172 (1990); magnetic tape data.
5. J. Sugar and C. Corliss, "Atomic energy levels of the iron-period elements: K through Ni," J. Phys. Chem. Ref. Data **14,** Suppl. 2 (1985).
6. J. E. Lawler in *Lasers, Spectroscopy, and New Ideas: A Tribute to Arthur L. Schawlow,* W. M. Yen and M. D. Levenson, eds., Vol. 54 of the Springer Series in Optical Sciences (Springer, New York, 1988), p. 125–140.
7. D. W. Duquette and J. E. Lawler, "Radiative lifetimes in NbI," Phys. Rev. A **26,** 330–334 (1982).
8. S. Salih, J. E. Lawler, and W. Whaling, "Lifetimes, branching ratios, and transition probabilities in Co II," Phys. Rev. A **31,** 744–749 (1985).
9. G. C. Marsden, E. A. Den Hartog, J. E. Lawler, J. T. Dakin, and V. D. Roberts, "Radiative lifetimes of even- and odd-parity levels in Sc I and Sc II,"J. Opt. Soc. Am. B **5,** 606–613 (1988).
10. H. Figger, K. Siomos, and H. Walther, "Lifetime measurements in the Fe I spectrum using tunable dye laser excitation," Z. Phys. **270,** 371–376 (1974).
11. J. Marek, J. Richter, and H. J. Stahnke, "Radiatives lifetimes of some Fe I levels," Phys. Scr. **19,** 325–327 (1979).
12. P. Hannaford and R. M. Lowe, "Determination of atomic lifetimes using pulsed laser excitation of sputtered metal vapours," J. Phys. B **14,** L5–L9 (1981).
13. H. Figger, J. Heldt, K. Siomos, and H. Walther, "Lifetime measurements in the Co I and Fe I spectra using tunable dye laser excitation," Astron. Astrophys. **43,** 389–394 (1975).
14. J. Carlsson, L. Sturesson, and S. Svanberg, "Accurate time-resolved laser spectroscopy on sputtered metal atoms," Z. Phys. D **11,** 287–293 (1989).
15. K. Siomos, H. Figger, and H. Walther, "Lifetime measurements in the Fe I spectrum using stepwise excitation by dye lasers," Z. Phys. A **272,** 355–358 (1975).
16. J. W. Brault, "Rapid-scan high-resolution Fourier spectrometer for the visible," J. Opt. Soc. Am. **66,** 1081 (1976).
17. B. A. Palmer, M. V. Phillips, and R. Engleman, "The infrared emission spectrum of U and Th," Proc. Soc. Photo-Opt. Instrum. Eng. **380,** 415–435 (1983).
18. W. L. Wiese, J. W. Brault, K. Danzmann, V. Helbig, and M. Kock, "Unified set of atomic transition probabilities for neutral argon," Phys. Rev. A **39,** 2461–2471 (1989).
19. J. A. Fernley, K. T. Taylor, and M. J. Seaton, "Atomic data for opacity calculations," J. Phys. B **20,** 6457–6476 (1987).
20. L. M. Faires, B. A. Palmer, and J. W. Brault, "Line width and line shape analysis in the ICP by high-resolution FT spectrometry," Spectrochim. Acta **40B,** 135–145 (1985).
21. M. Kock, S. Kroll, and S. Schnehage, "Fe I oscillator strengths," Phys. Scri. **T8,** 84–87 (1984).
22. B. A. Palmer and R. Engleman, "A new program for the least squares calculation of atomic energy levels," Report LA-9710 (Los Alamos National Laboratory, Los Alamos, N. Mex., 1983).
23. J. W. Brault, in R. S. Booth, J. W. Brault, and A. Labeyrie, *High Resolution in Astronomy* (Geneva Observatory, Geneva, 1985).
24. R. C. M. Learner and A. P. Thorne, "Wavelength calibration of Fourier transform emission spectra with applications to Fe I," J. Opt. Soc. Am. B **5,** 2045–2059 (1988).
25. G. Norlén, "Wavelengths and energy levels of Ar I and Ar II based on new interferometric measurements in the region 3400–9800 Å," Phys. Scr. **8,** 249–268 (1973).
26. C. M. Brown, M. L. Ginter, S. Johansson, and S. G. Tilford, "Absorption spectra of Fe I in the 1550–3215-Å region," J. Opt. Soc. Am. B **5,** 2125–2158 (1988).
27. S. E. Johansson, Department of Physics, University of Lund, Sölvegatan 14, S223 62 Lund, Sweden (personal communication).